



Stochastic modeling of the oceanic mesoscale eddies

Long Li, Deremble Bruno, Noé Lahaye, Etienne Mémin

► To cite this version:

Long Li, Deremble Bruno, Noé Lahaye, Etienne Mémin. Stochastic modeling of the oceanic mesoscale eddies. STUOD 2021 - 6th Sandbox Stochastic Transport in Upper Ocean Dynamics Workshop, Feb 2021, London, United Kingdom. pp.1-24. hal-03140513

HAL Id: hal-03140513

<https://inria.hal.science/hal-03140513>

Submitted on 15 Feb 2021

HAL is a multi-disciplinary open access archive for the deposit and dissemination of scientific research documents, whether they are published or not. The documents may come from teaching and research institutions in France or abroad, or from public or private research centers.

L'archive ouverte pluridisciplinaire **HAL**, est destinée au dépôt et à la diffusion de documents scientifiques de niveau recherche, publiés ou non, émanant des établissements d'enseignement et de recherche français ou étrangers, des laboratoires publics ou privés.



Stochastic modeling of the oceanic mesoscale eddies

The 6th STUDO Sandbox Workshop – 12 February 2021

Long Li¹, Bruno Deremble², Noé Lahaye¹ and Etienne Mémin¹

¹ Inria Rennes Bretagne Atlantique, France

² Institut des Géosciences de l'Environnement, France

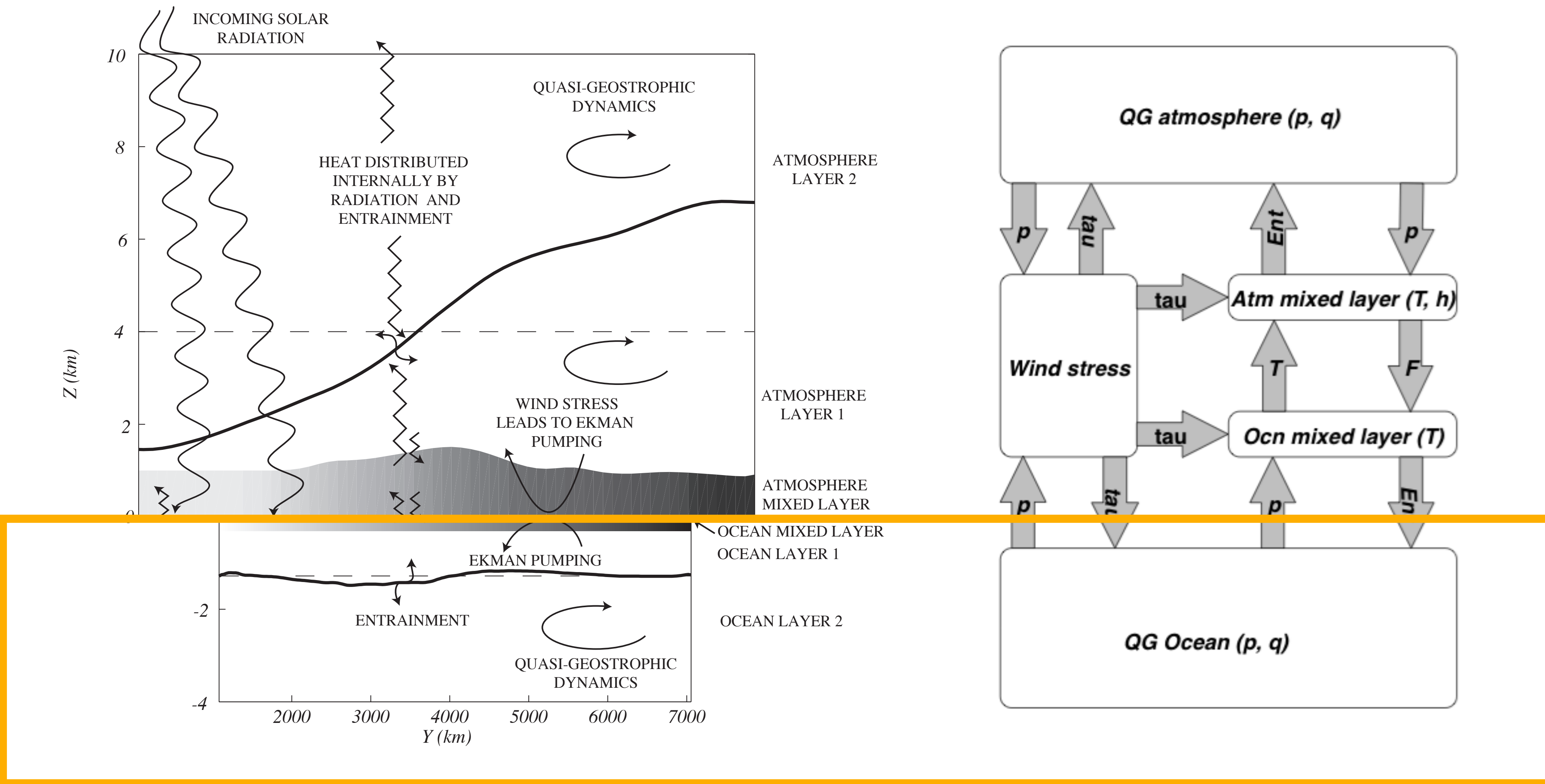




Motivations

- I. Can LU model better represent the mesoscale eddies effect on the large-scale circulation?
- II. Can LU model improve the internal variability of coarse-resolution ocean models?

Dynamical core



Quasi-Geostrophic Coupled Model (Q-GCM) [<http://q-gcm.org>]

Deterministic QG equations

- Evolution of k -th layer potential vorticity (PV)

$$\partial_t q_k = -\nabla \cdot (\mathbf{u}_k q_k) + \frac{A_2}{f_0} \nabla^4 p_k - \frac{A_4}{f_0} \nabla^6 p_k - \frac{f_0}{H_k} (w_k - w_{k-1})$$

- Update k -th layer pressure, height and velocity

$$q_k = \frac{1}{f_0} \nabla^4 p_k + \beta(y - y_0) + \frac{f_0}{H_k} (\eta_k - \eta_{k-1})$$

$$\eta_k = \frac{p_{k+1} - p_k}{g'_k}, \quad g'_k = \frac{g(\rho_{k+1} - \rho_k)}{\rho_0}$$

$$\mathbf{u}_k = \frac{1}{f_0} \nabla^\perp p_k$$

Exp.1

- Evolution of mixed layer temperature (or SST)

$$\mathbf{u}_m = \mathbf{u}_1 + \frac{\boldsymbol{\tau}^\perp}{f_0 H_m}$$

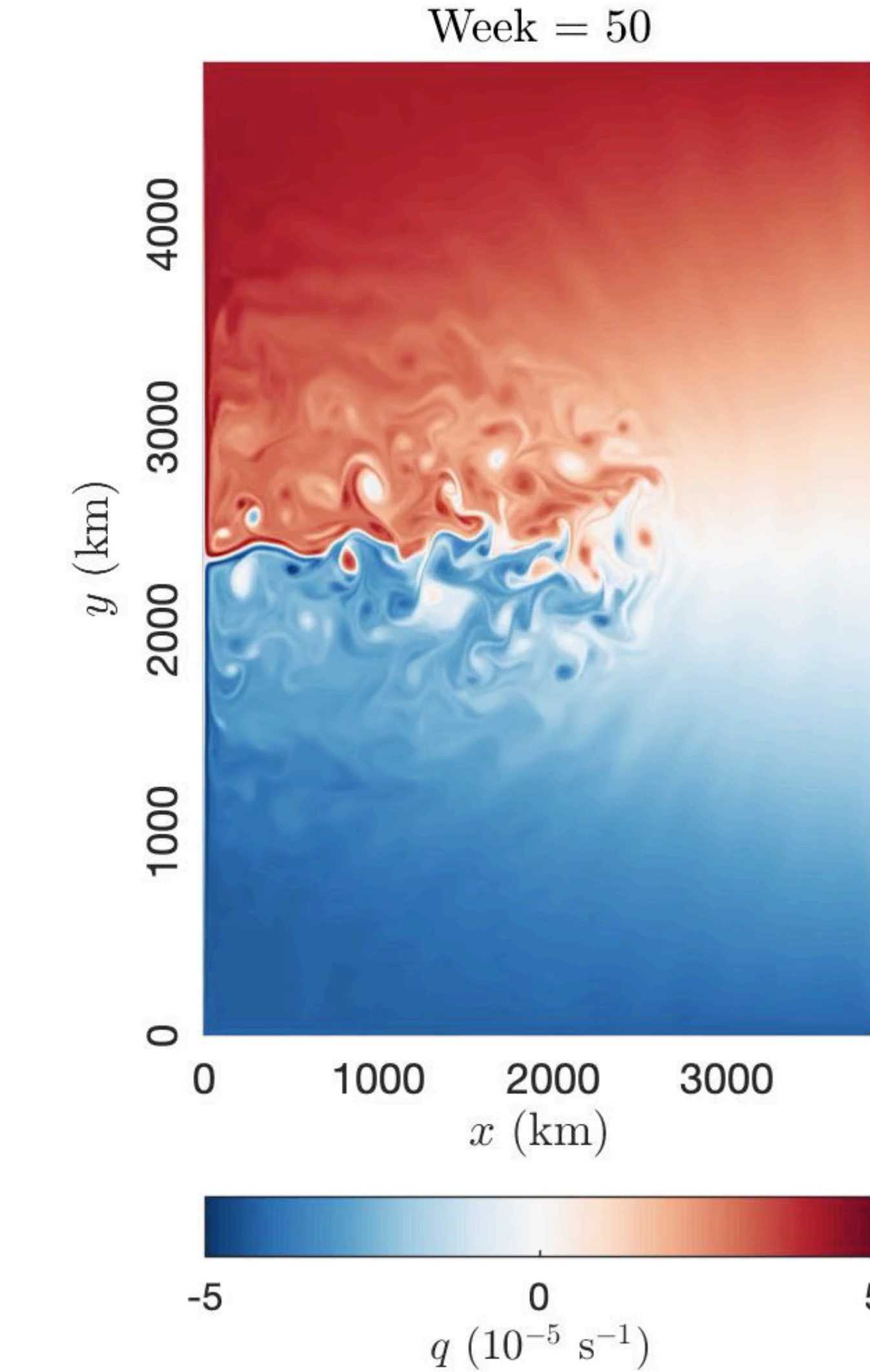
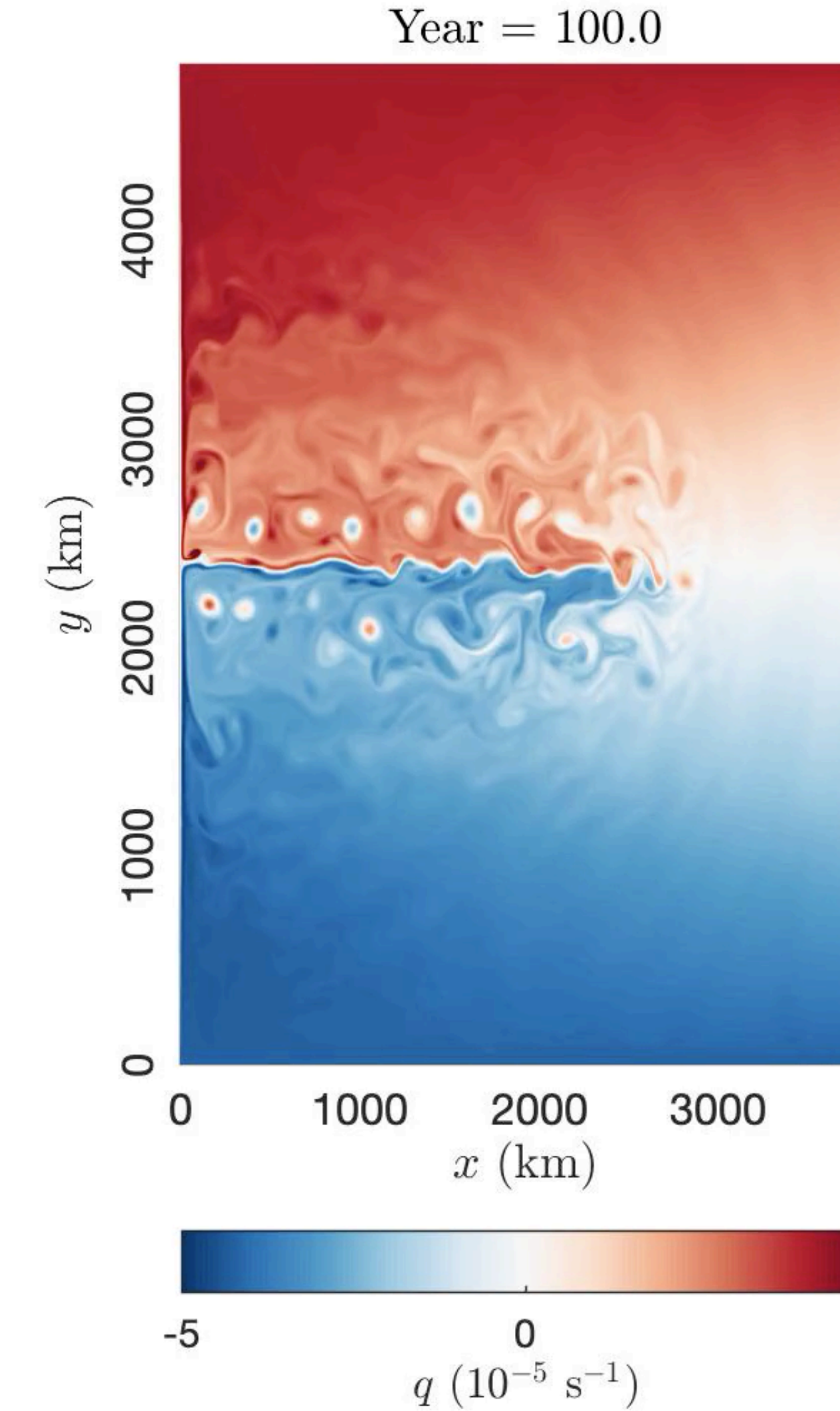
$$\partial_t T_m = -\nabla \cdot (\mathbf{u}_m T_m) + K_2 \nabla^2 T_m - K_4 \nabla^4 T_m + w_0 \frac{T_1 + T_m}{2H_m} - F_m$$

$$w_1 = -\frac{\Delta_m T}{2\Delta_1 T} w_0$$

Exp.2

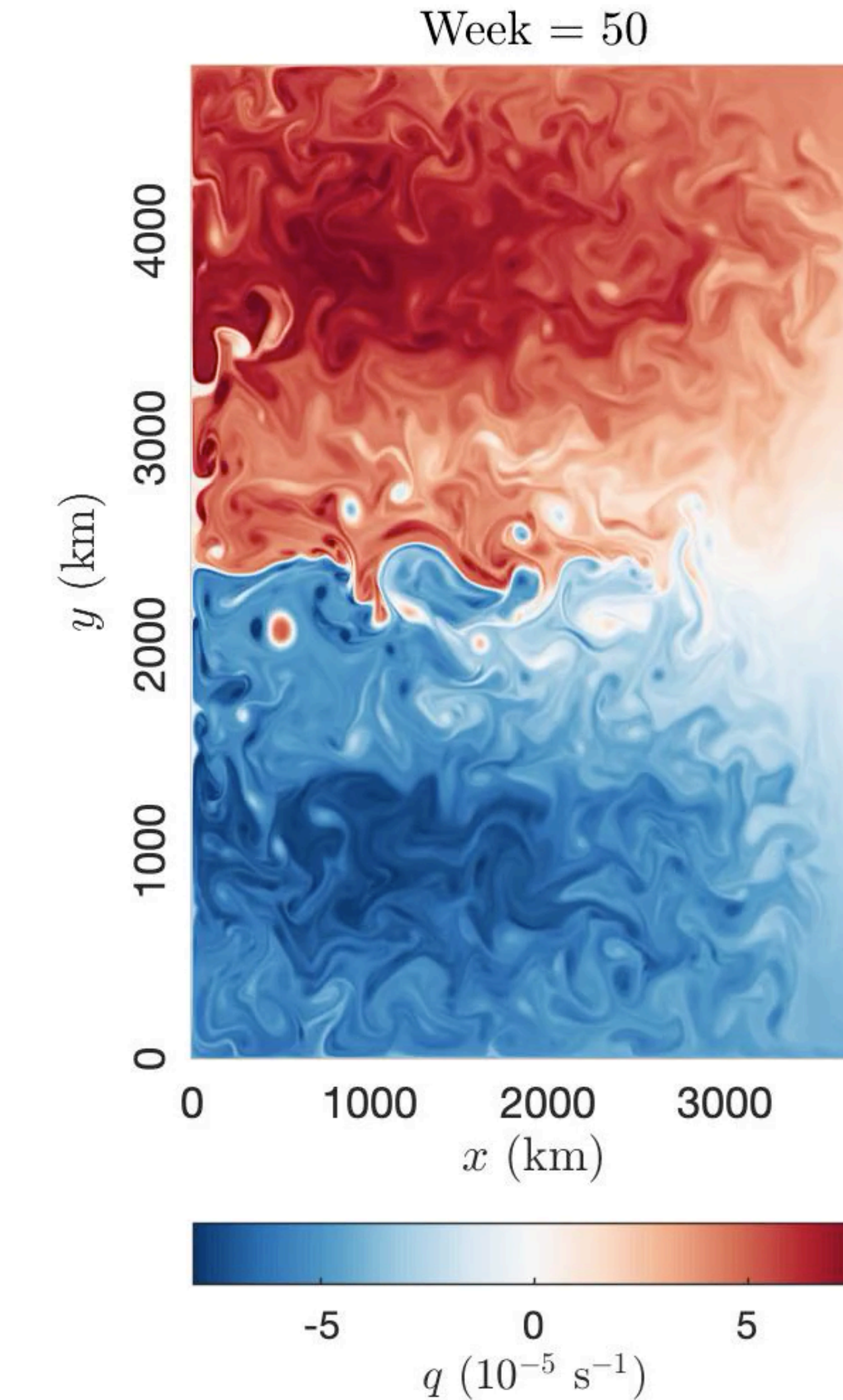
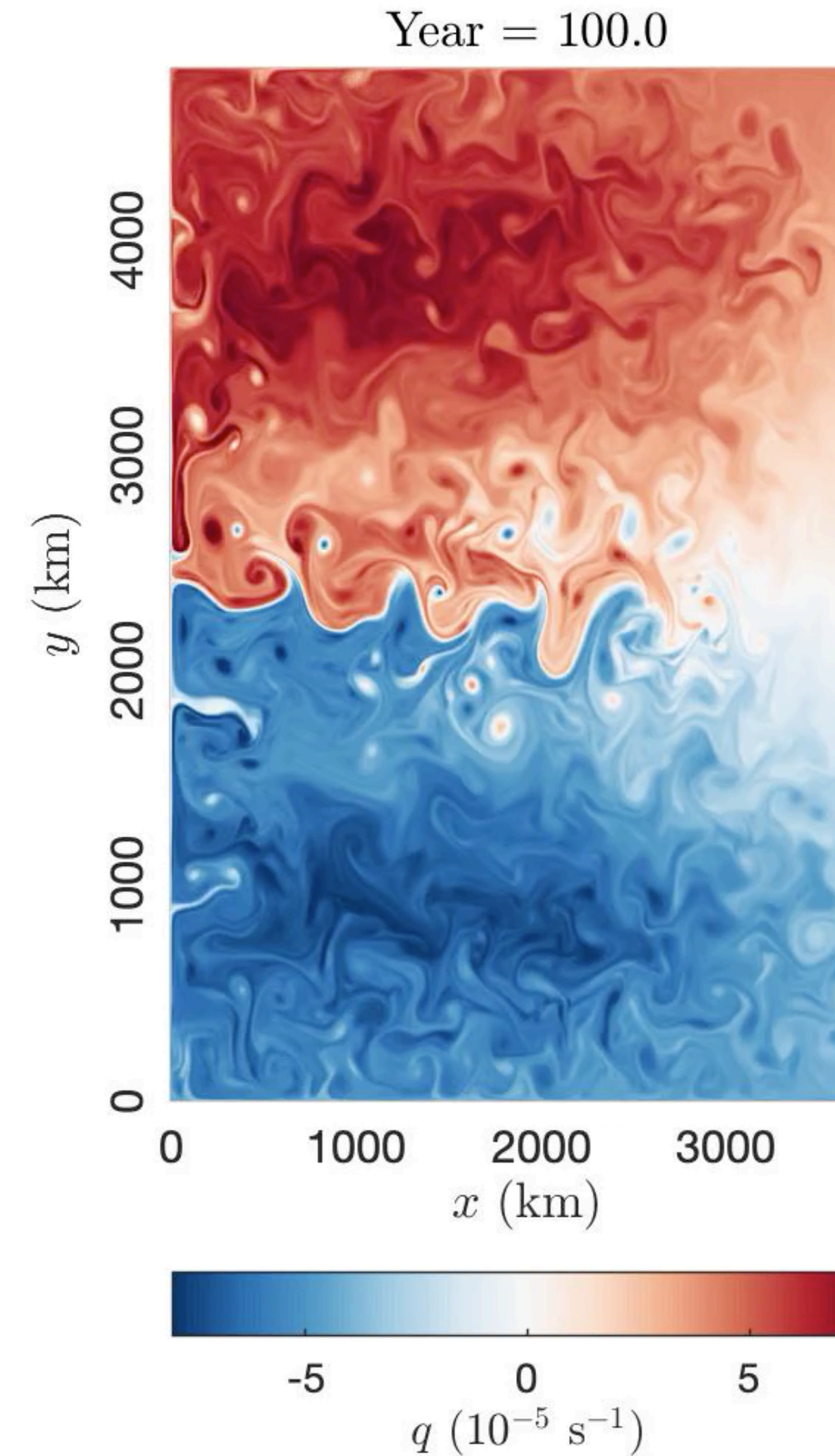
$$\left[\begin{array}{l} w_0 = \frac{1}{f_0} \nabla \times \boldsymbol{\tau} \\ w_N = \frac{\delta_{ek}}{2f_0} \nabla^2 p_N \end{array} \right]$$

Eddy-resolving simulations



Upper-layer PV ($\Delta x = 5$ km, $L_d = [39,22]$ km) of Exp.1 (without SST)

Eddy-resolving simulations



Upper-layer PV ($\Delta x = 5$ km, $L_d = [39,22]$ km) of Exp.2 (with SST)

Stochastic QG equations

- **k -th layer eddy velocity noise (m/s)** $\sigma_k \dot{B}_t$
- **k -th layer variance tensor (m²/s²)** $\frac{a_k}{dt} = \mathbb{E}\left[\left(\sigma_k \dot{B}_t - \mathbb{E}[\sigma_k \dot{B}_t]\right)\left(\sigma_k \dot{B}_t - \mathbb{E}[\sigma_k \dot{B}_t]\right)^T\right]$
- **Evolution of k -th layer PV** $\partial_t q_k = -\nabla \cdot (\mathbf{u}_k q_k) + \frac{A_2}{f_0} \nabla^4 p_k - \frac{A_4}{f_0} \nabla^6 p_k - \frac{f_0}{H_k} (w_k - w_{k-1}) + \nabla \cdot F_k$

$F_k = -\left(\sigma_k \dot{B}_t - \frac{1}{2} \nabla \cdot \mathbf{a}_k\right) q_k + \frac{1}{2} \mathbf{a}_k \nabla q_k - \left(\mathbf{u}_k \cdot \nabla^\perp \sigma_k \dot{B}_t + \mathbf{a}_k \nabla f\right) + \frac{1}{2} \sum_{i=1,2} \partial_{x_i}^\perp \mathbf{a}_k \nabla u_k^i$

Advection flux **Diffusion flux** **Sources flux** **Sinks flux**
- **Evolution of SST** $\partial_t T_m = -\nabla \cdot (\mathbf{u}_m T_m) + K_2 \nabla^2 T_m - K_4 \nabla^4 T_m + w_0 \frac{T_1 + T_m}{2H_m} - F_m + \nabla \cdot F_m$

$F_m = -\left(\sigma_1 \dot{B}_t - \frac{1}{2} \nabla \cdot \mathbf{a}_1\right) T_m + \frac{1}{2} \mathbf{a}_1 \nabla T_m$

Data-driven modeling

(i) LU-POD

$$\mathbf{u}_k^{\text{HR}} - \overline{\mathbf{u}_k^{\text{HR}}} = \mathcal{F}\mathbf{u}_k^{\text{HR}} + (1 - \mathcal{F})\mathbf{u}_k^{\text{HR}} - \overline{\mathcal{F}\mathbf{u}_k^{\text{HR}}} + (1 - \mathcal{F})\mathbf{u}_k^{\text{HR}}$$

$$= (\mathbf{u}_k^{\text{LR}} - \overline{\mathbf{u}_k^{\text{LR}}}) + (1 - \mathcal{F})\mathbf{u}_k^{\text{HR}} - \overline{(1 - \mathcal{F})\mathbf{u}_k^{\text{HR}}}$$

POD

$$\{\phi_{k,n}\}_{n=1,\dots,N_t}$$

$$\mathbf{u}_k^* = -\mathcal{F}\overline{(1 - \mathcal{F})\mathbf{u}_k^{\text{HR}}}$$

$$[\mathbf{u}_k^* \neq 0 \text{ if } \mathcal{F}^2 \neq \mathcal{F}]$$

$$\begin{aligned} \xi_n &\sim \mathcal{N}(0, 1) \\ (M_0 < M_1 < N_t) \end{aligned}$$

$$\sigma_k \dot{B}_t = \sum_{n=M_0}^{M_1} \phi_{k,n} \xi_n + \mathbf{u}_k^*$$

$$\frac{d}{dt} \mathbf{a}_k = \sum_{n=M_0}^{M_1} \phi_{k,n} \phi_{k,n}^T$$

Data-driven modeling

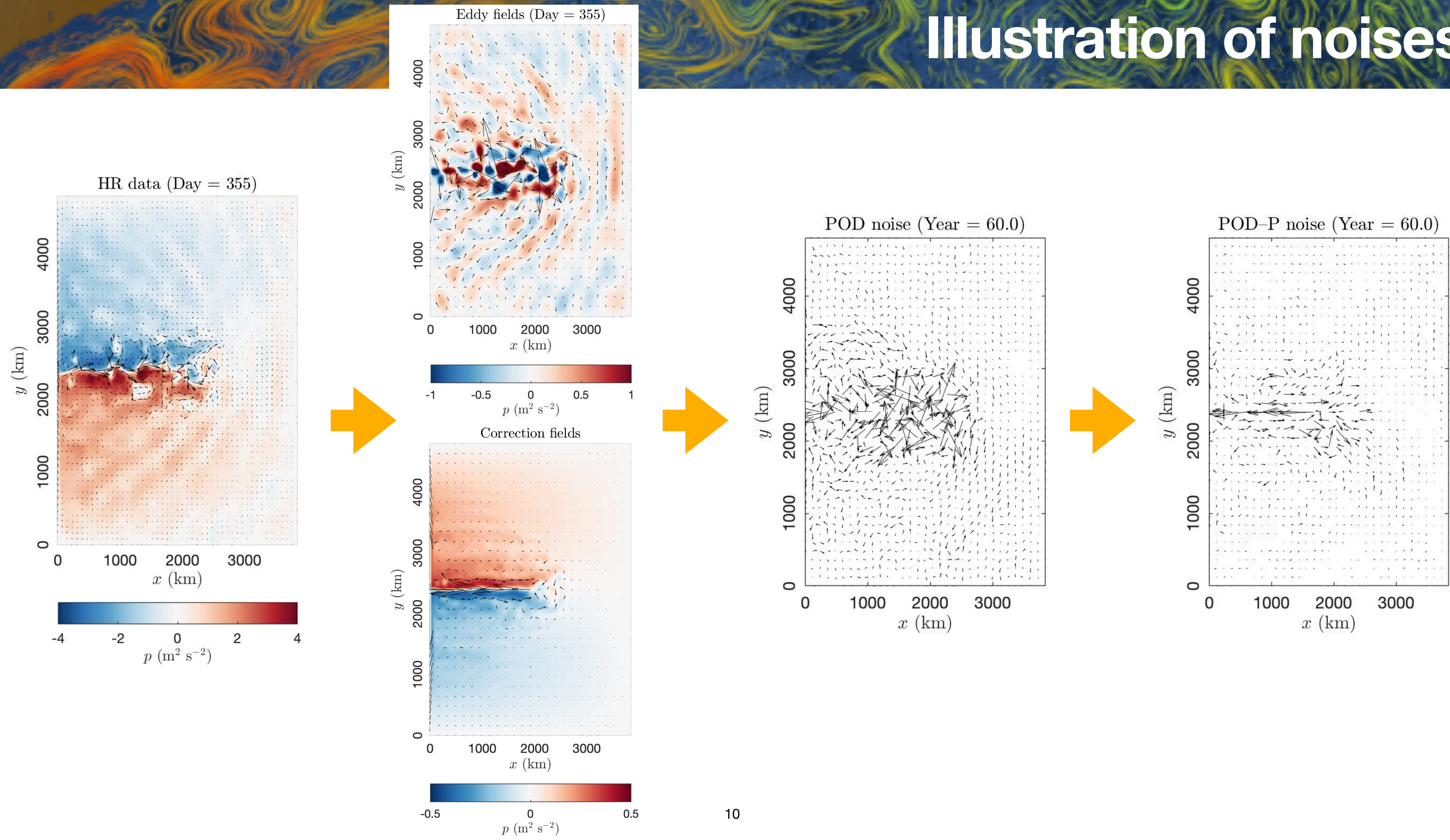
(ii) LU-POD-P

$$\mathbf{P}_k = \mathbf{I} - \frac{\nabla\theta_k(\nabla\theta_k)^T}{\|\nabla\theta_k\|^2}, \quad \theta_k = \frac{f_0}{H_k}(\eta_k - \eta_{k-1})$$

$$\tilde{\boldsymbol{\sigma}}_k \dot{\boldsymbol{B}}_t = \mathbf{P}_k \boxed{\boldsymbol{\sigma}_k \dot{\boldsymbol{B}}_t}, \quad \tilde{\boldsymbol{a}}_k = \mathbf{P}_k \boldsymbol{a}_k \mathbf{P}_k^T$$

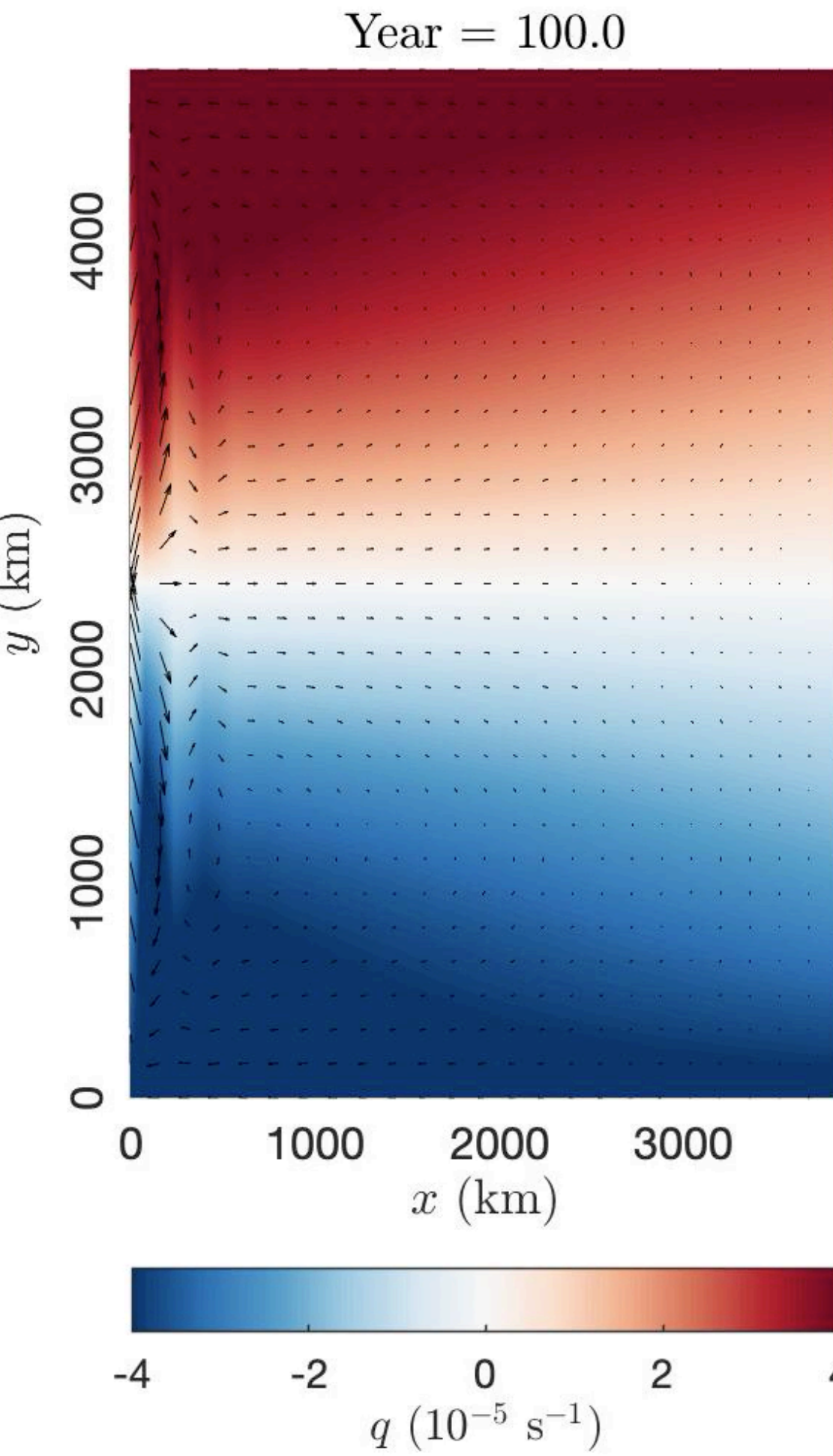
LU-POD

Illustration of noises

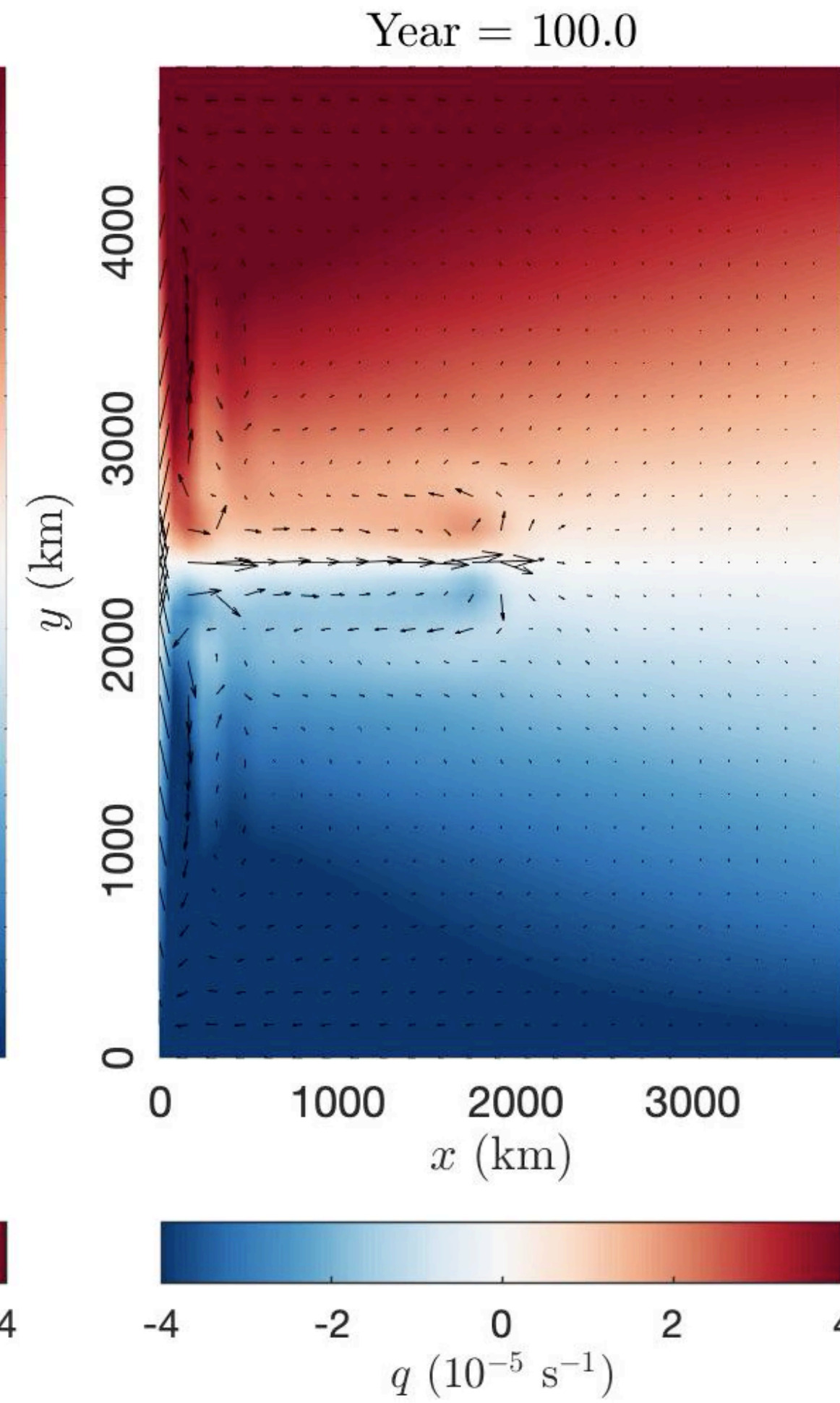


Coarse-resolution simulations

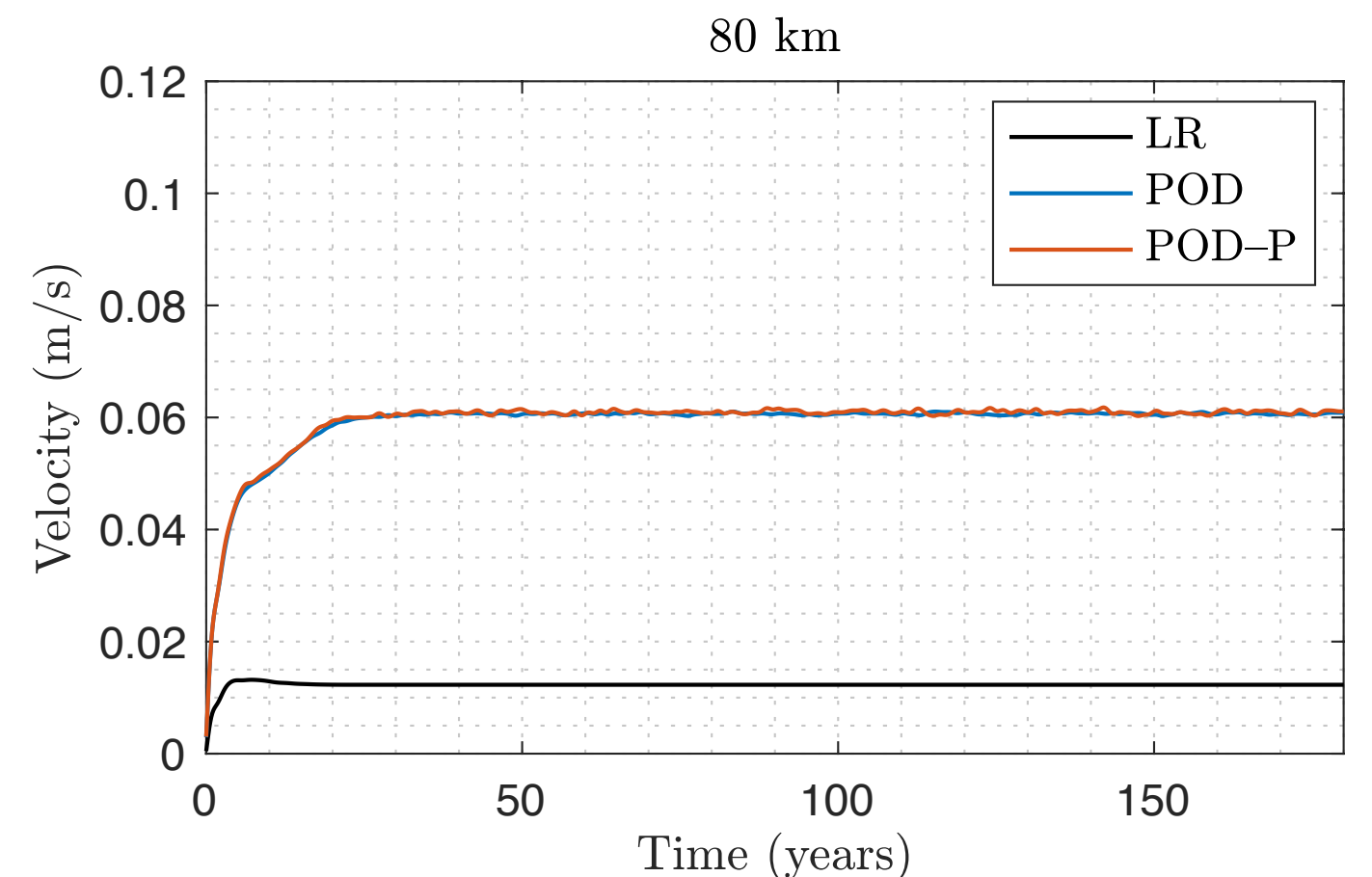
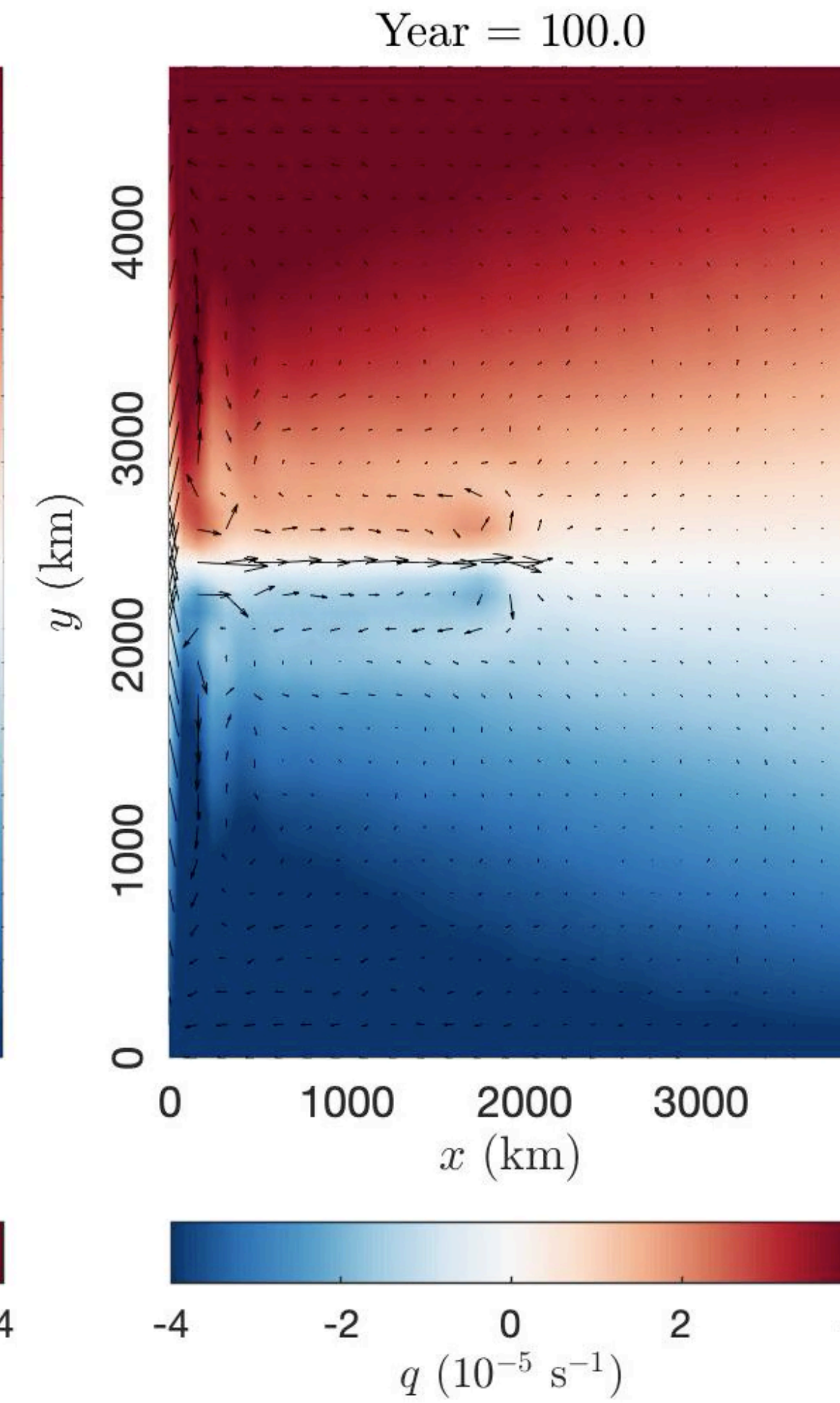
LR



LU-POD



LU-POD-P



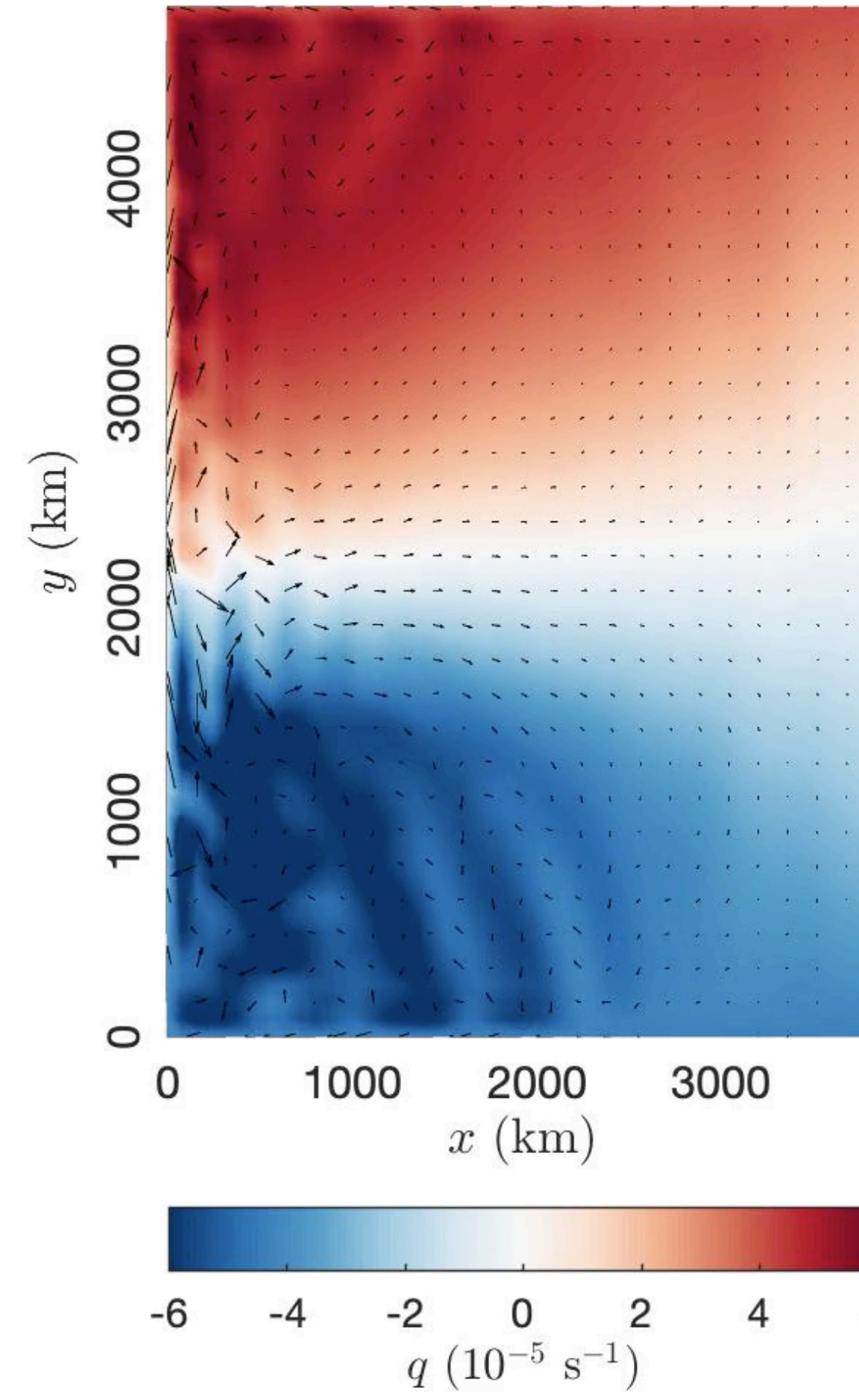
Comparison of jet velocity magnitude

Upper-layer PV ($\Delta x = 80 \text{ km}$, $L_d = [39, 22] \text{ km}$) of Exp.1 (without SST)

Coarse-resolution simulations

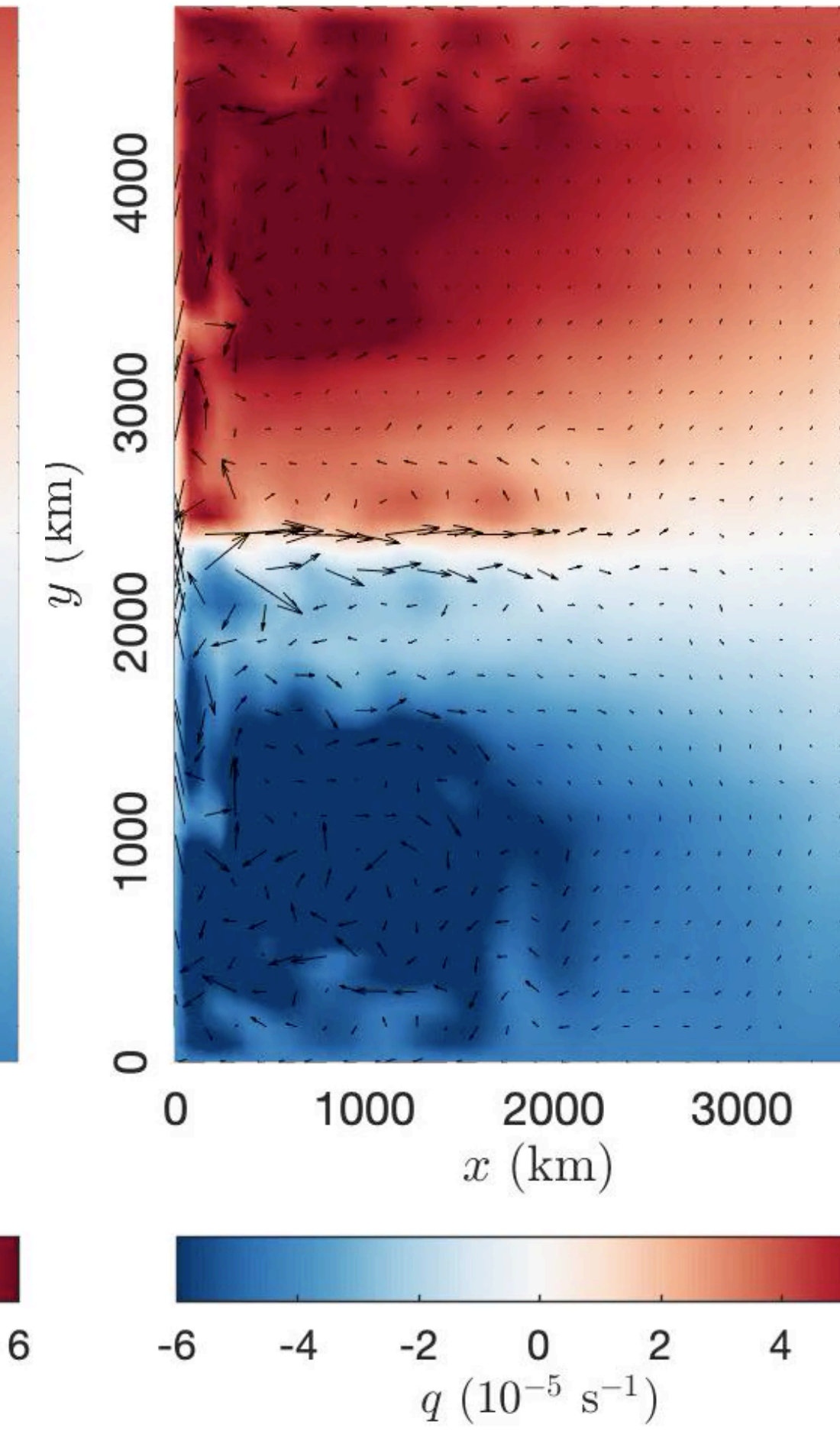
LR

Year = 100.0



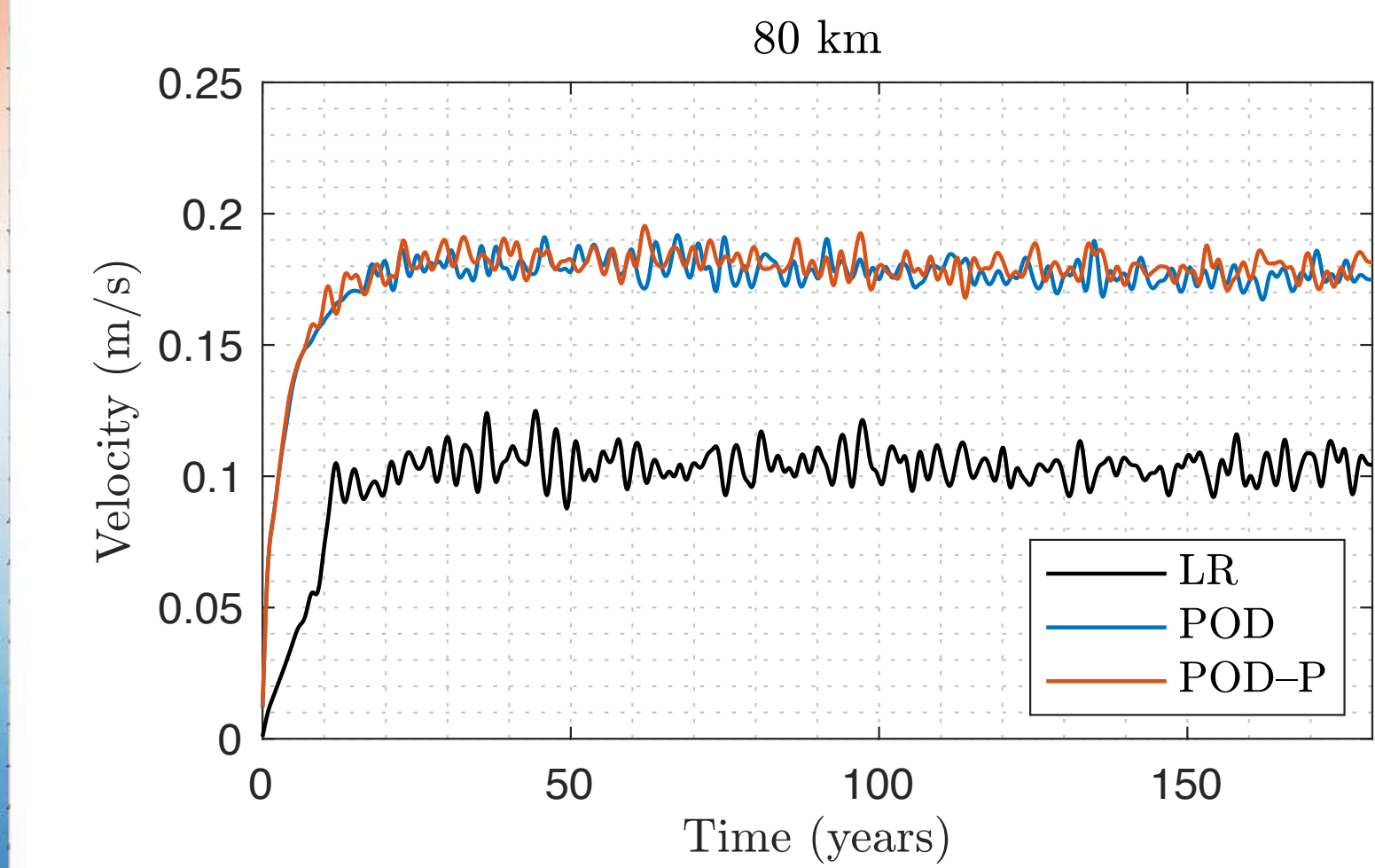
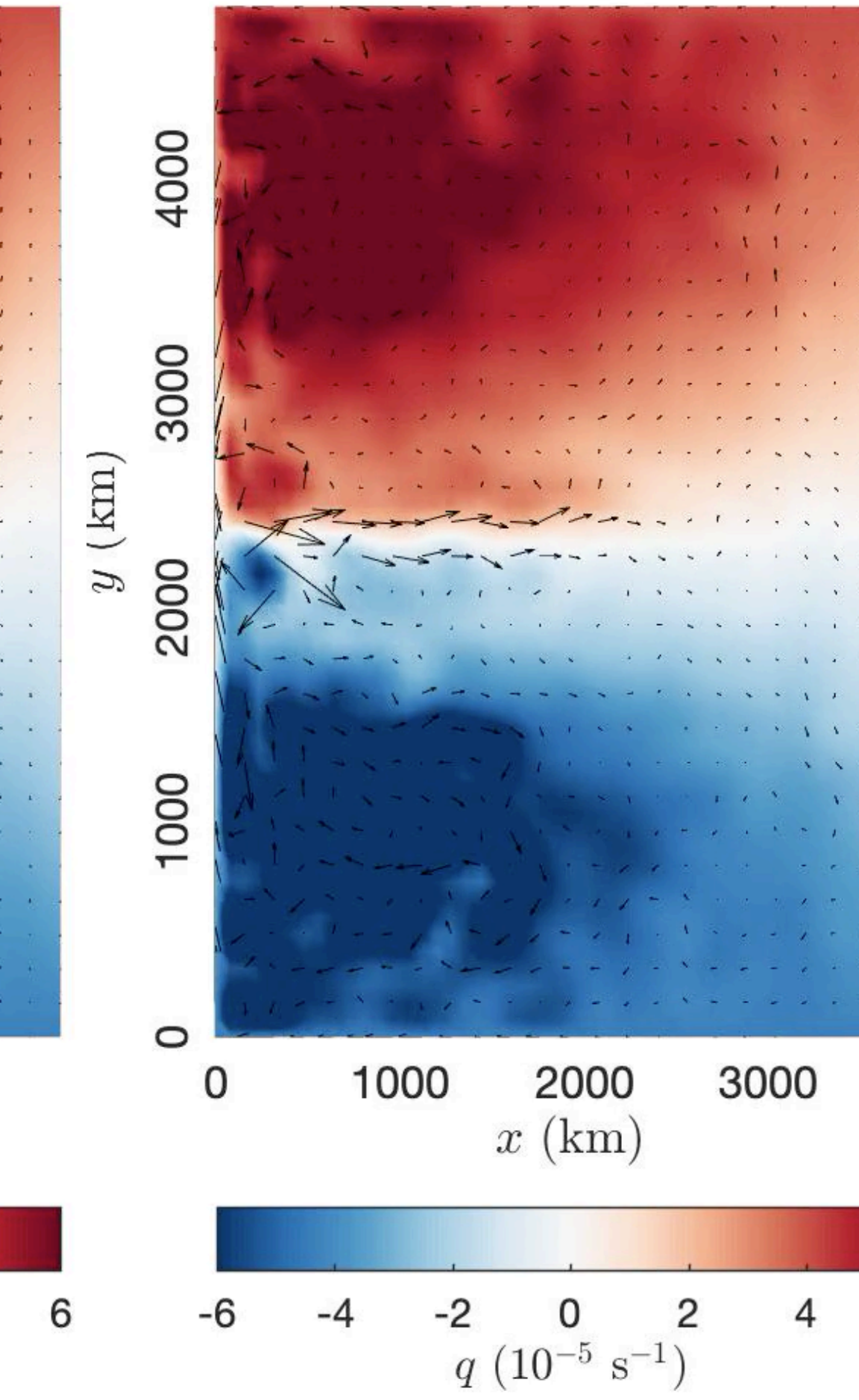
LU-POD

Year = 100.0



LU-POD-P

Year = 100.0

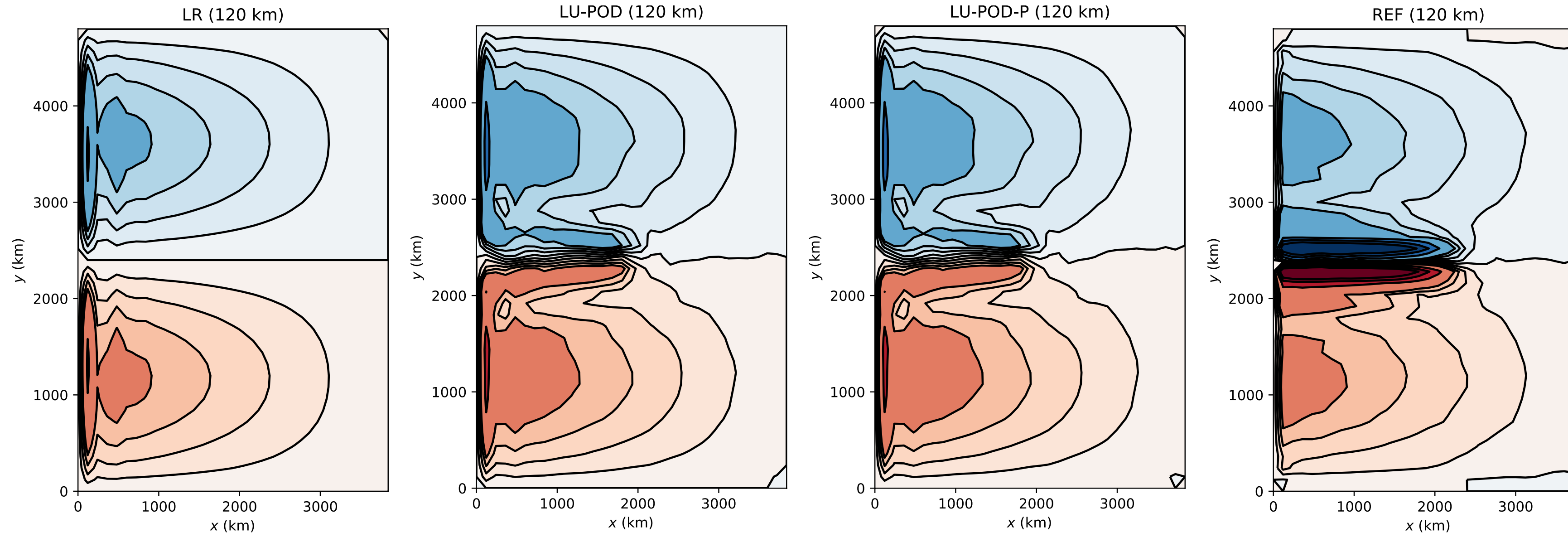


Comparison of jet velocity magnitude

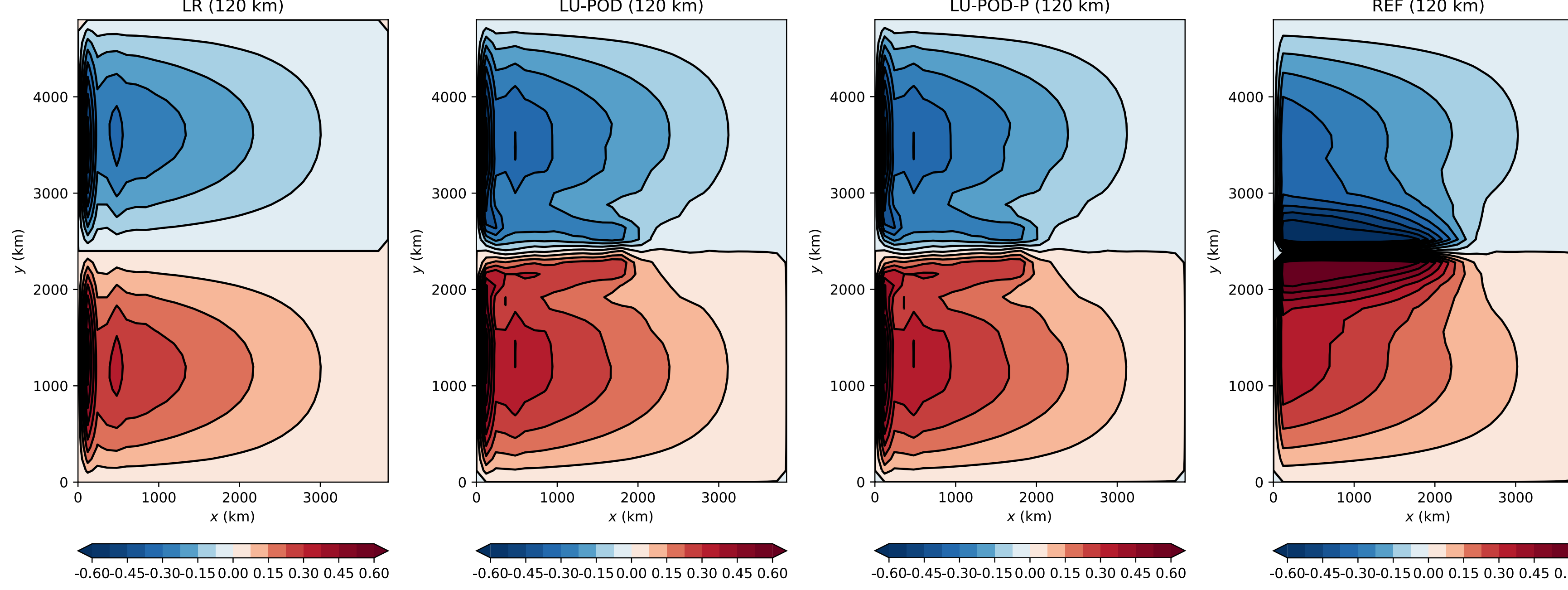
Upper-layer PV ($\Delta x = 80$ km, $L_d = [39,22]$ km) of Exp.2 (with SST)

Statistical prediction

Barotropic mode



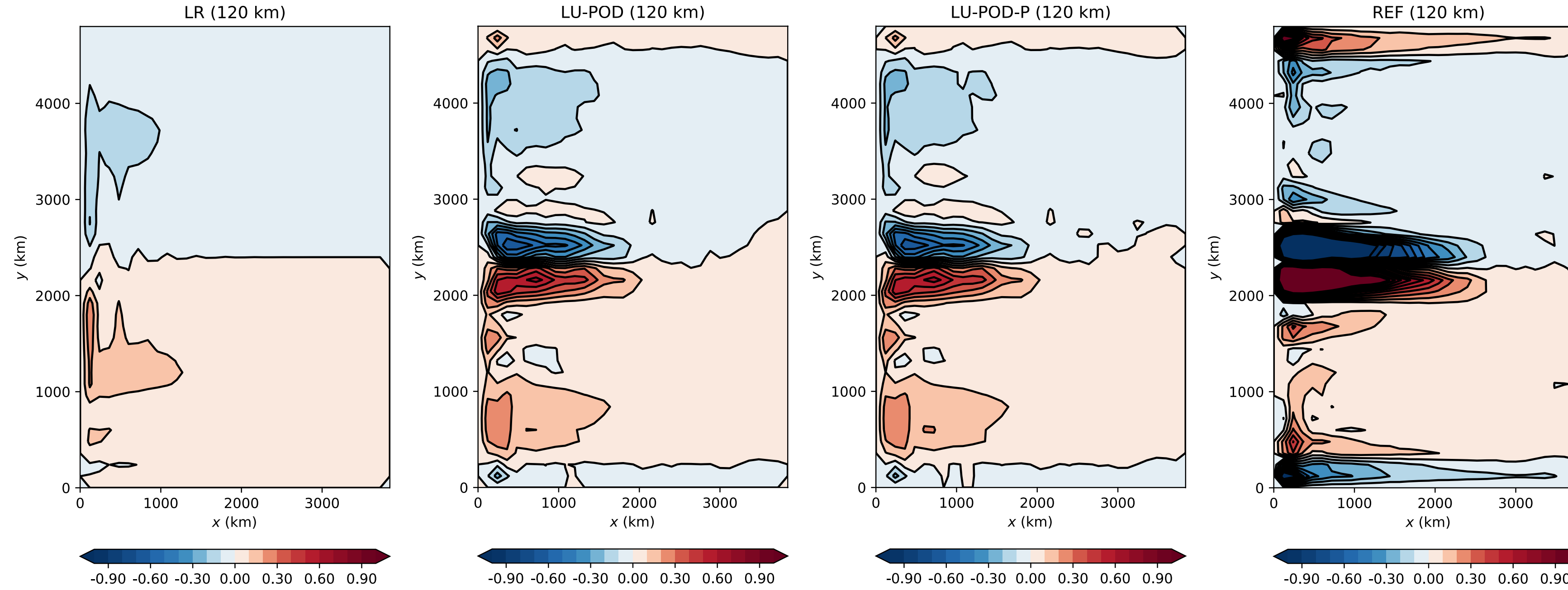
1st Baroclinic mode



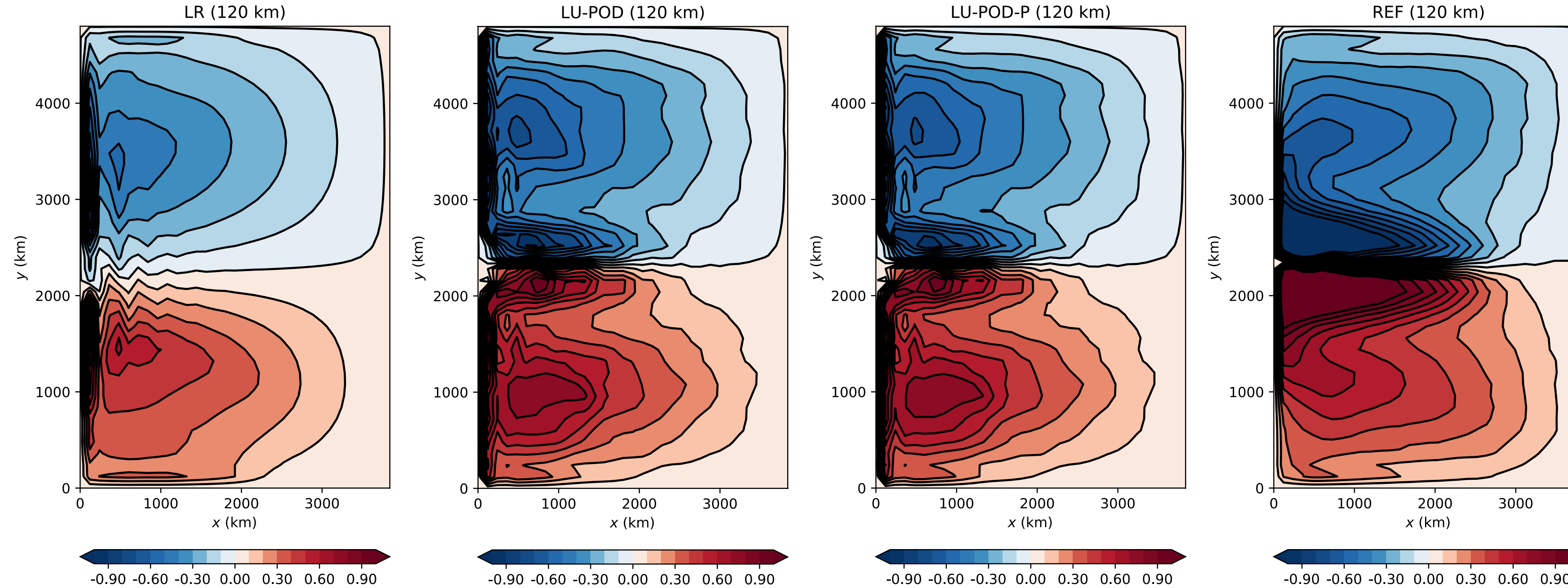
Comparison of
mean (60-180
yrs) contour of
pressure for
coarse-model
(120 km)
simulations
(Exp.1)

Statistical prediction

Barotropic mode



1st Baroclinic mode



Comparison of
mean (60-180
yrs) contour of
pressure for
coarse-model
(120 km)
simulations
(Exp.2)

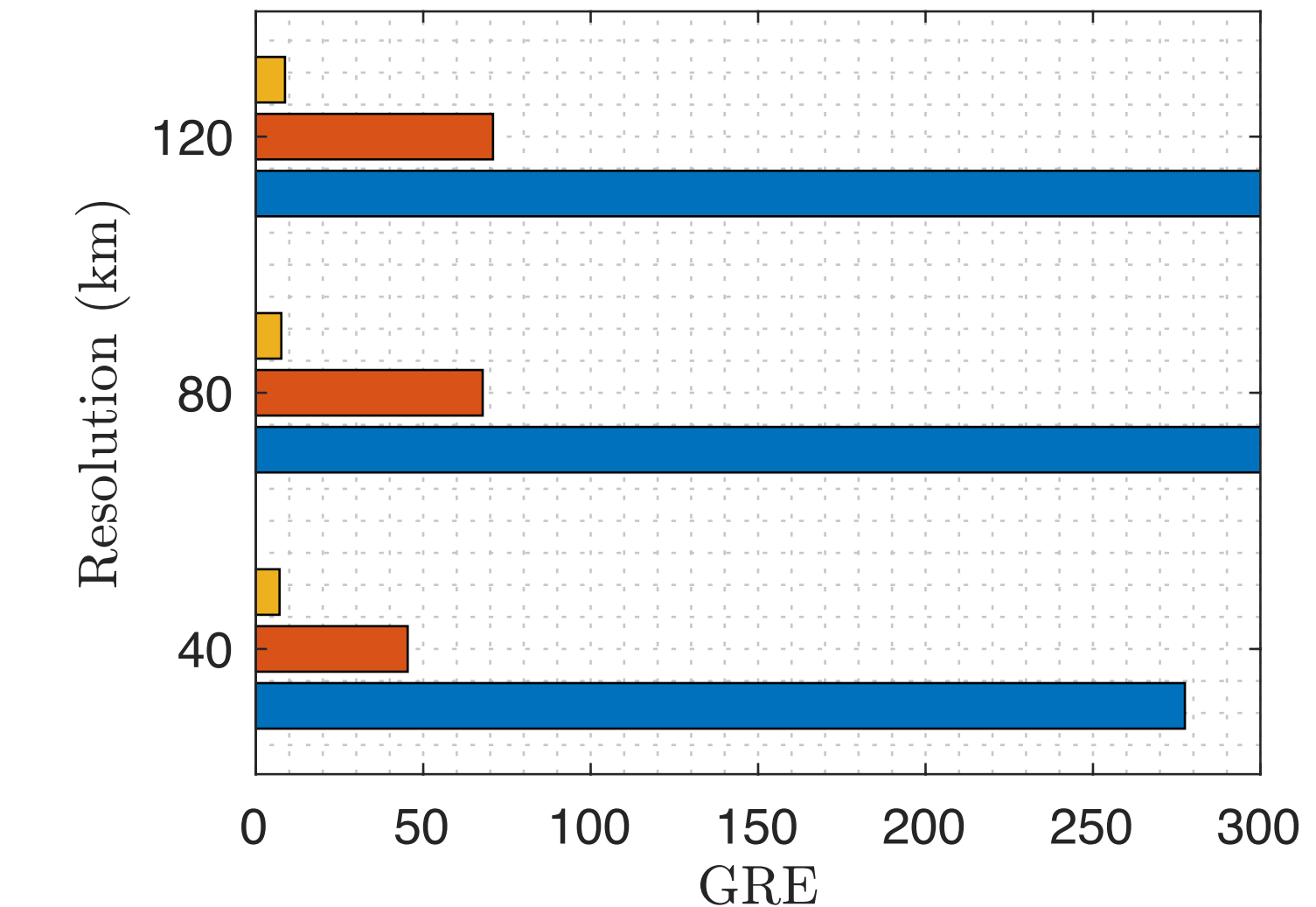
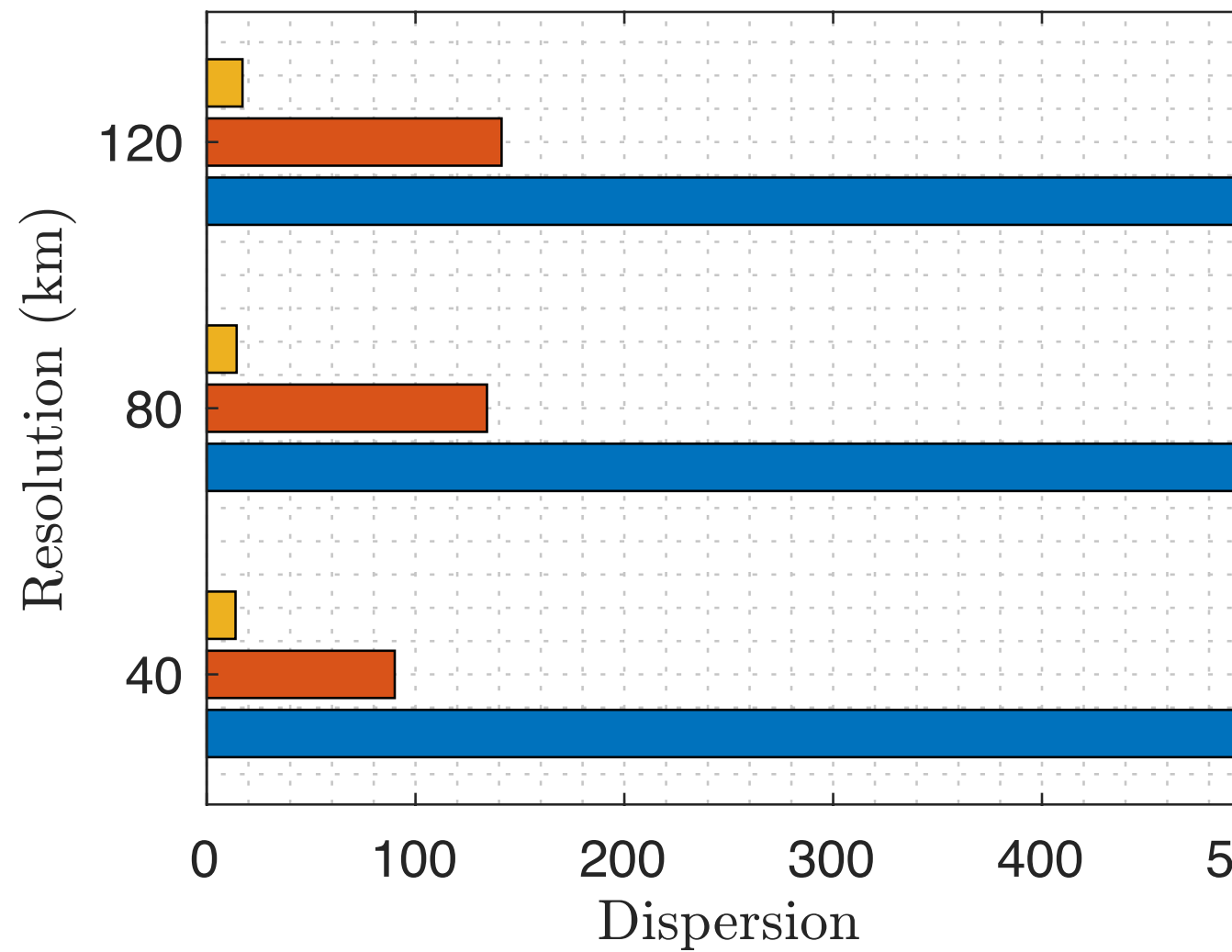
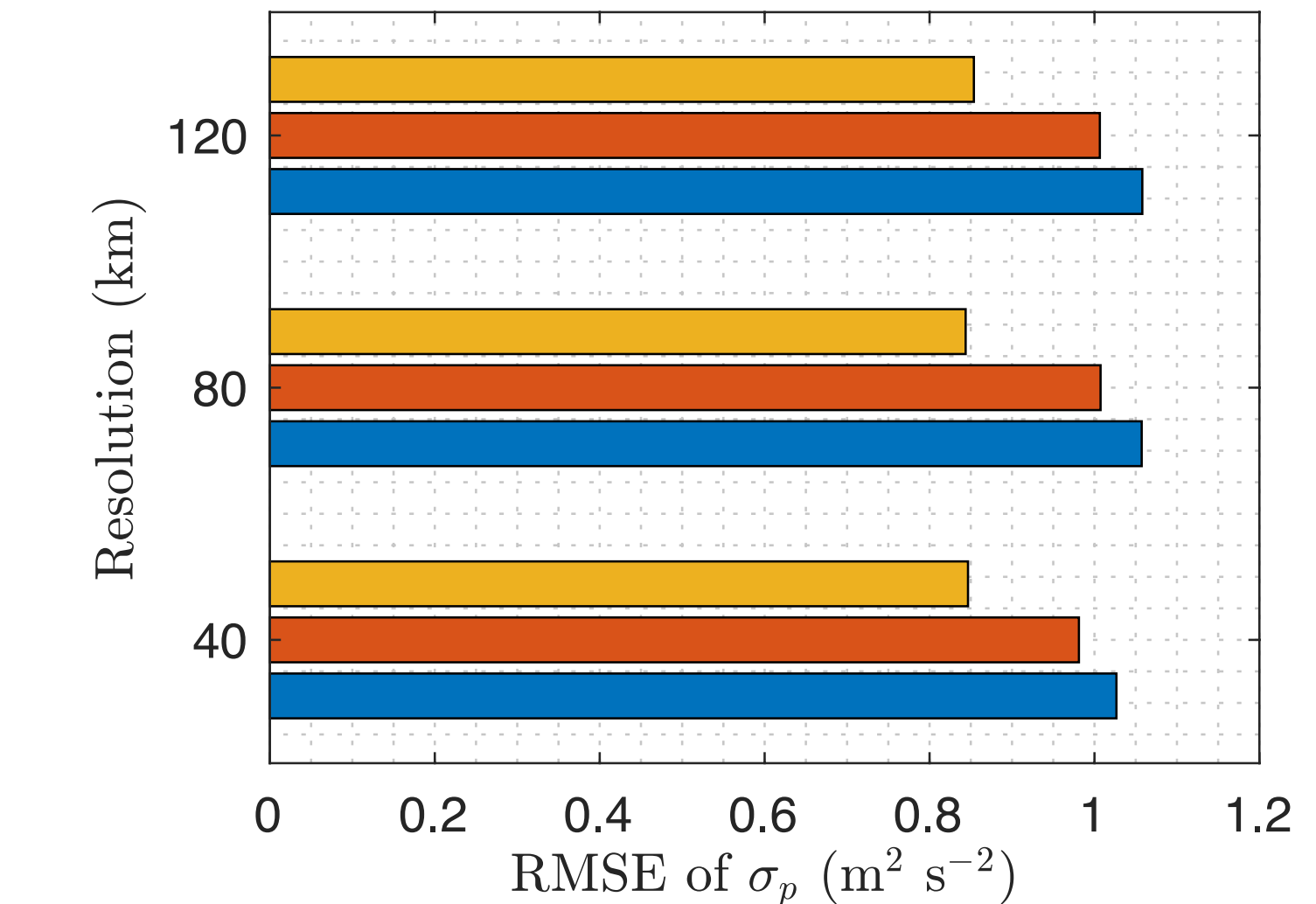
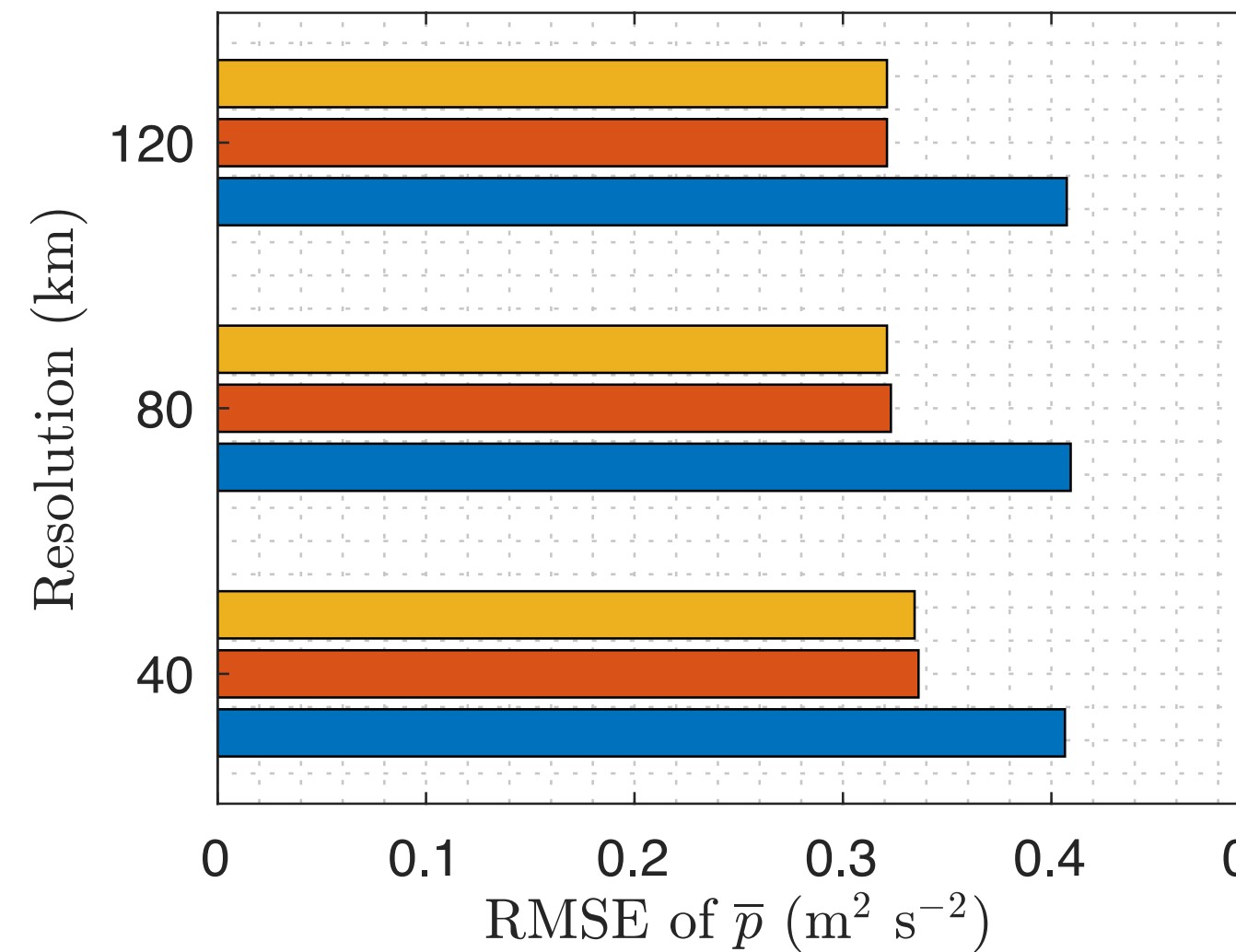
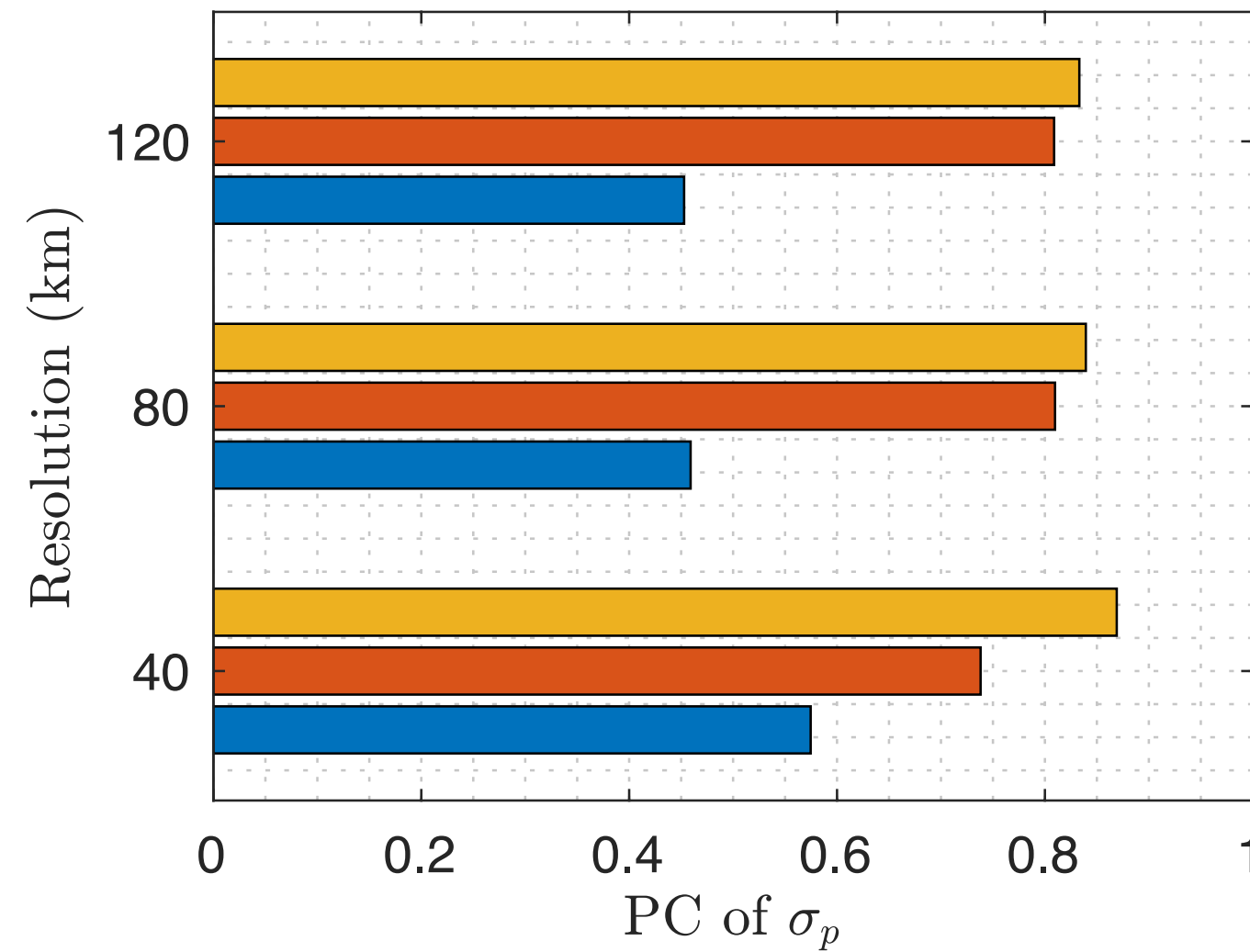
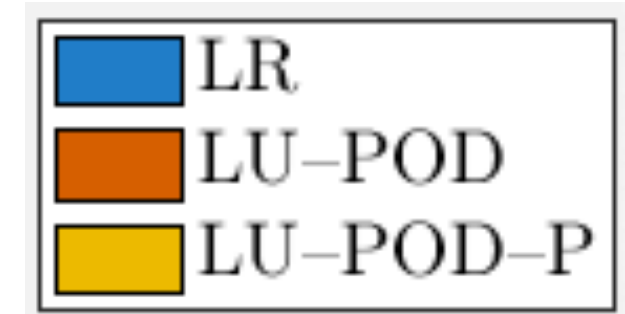
Measures of statistics

Measures	Values	Accuracy
$\text{RMSE of } \bar{p}_{\text{MOD}} = \ \bar{p}_{\text{MOD}} - \bar{p}_{\text{REF}}\ _A$	↓	+
$\text{RMSE of } \sigma_{\text{MOD}} = \ \sigma_{\text{MOD}} - \sigma_{\text{REF}}\ _A, \quad \sigma = \overline{(p - \bar{p})^2}$	↓	+
$\text{PC} = \frac{\ \sigma_{\text{REF}} \sigma_{\text{MOD}}\ _A^2}{\ \sigma_{\text{REF}}^2\ _A \ \sigma_{\text{MOD}}^2\ _A}$	↗	+
$\text{Dispersion} = \frac{1}{ A } \int \int \left(\frac{\sigma_{\text{REF}}^2}{\sigma_{\text{MOD}}^2} - 1 - \log \left(\frac{\sigma_{\text{REF}}^2}{\sigma_{\text{MOD}}^2} \right) \right) dA$	↓	+
$\text{GRE} = \frac{1}{2} \left\ \frac{\bar{p}_{\text{REF}} - \bar{p}_{\text{MOD}}}{\sigma_{\text{REF}}} \right\ _A^2 + \frac{1}{2} \text{Dispersion}$	↓	+

$$\|f\|_A = \left(\frac{1}{|A|} \int \int f^2 dA \right)^{1/2}$$

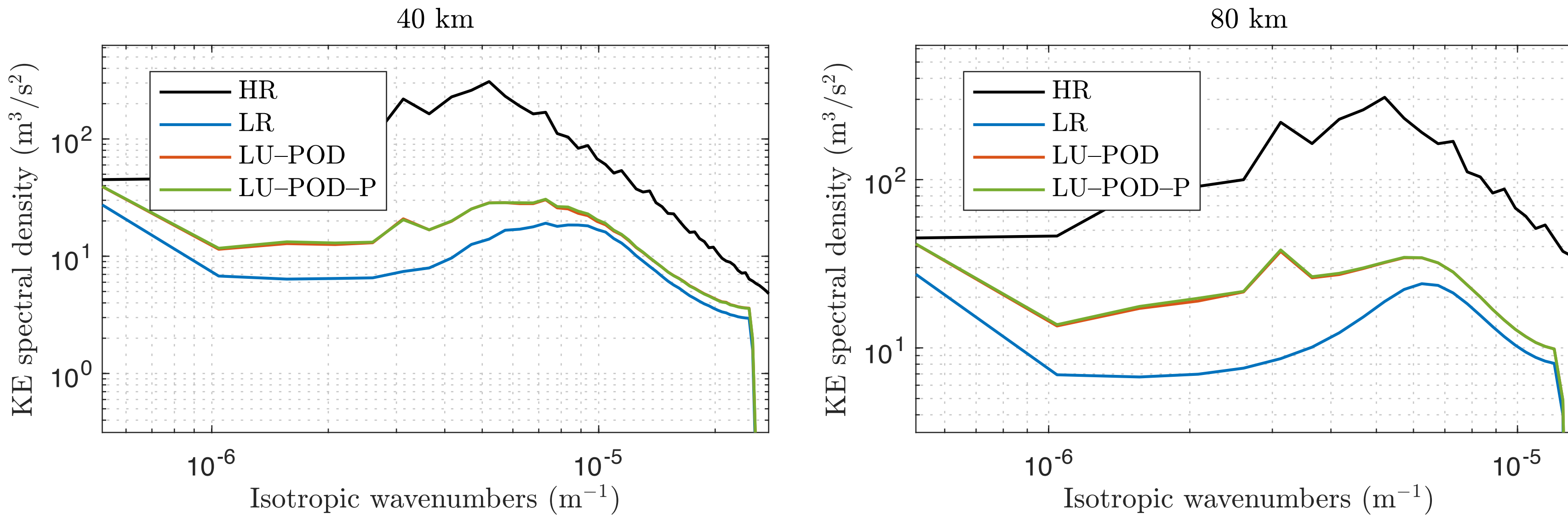
Statistical prediction

Comparison of statistical measures (integrated vertically) for pressures provided by different coarse models (Exp.2)

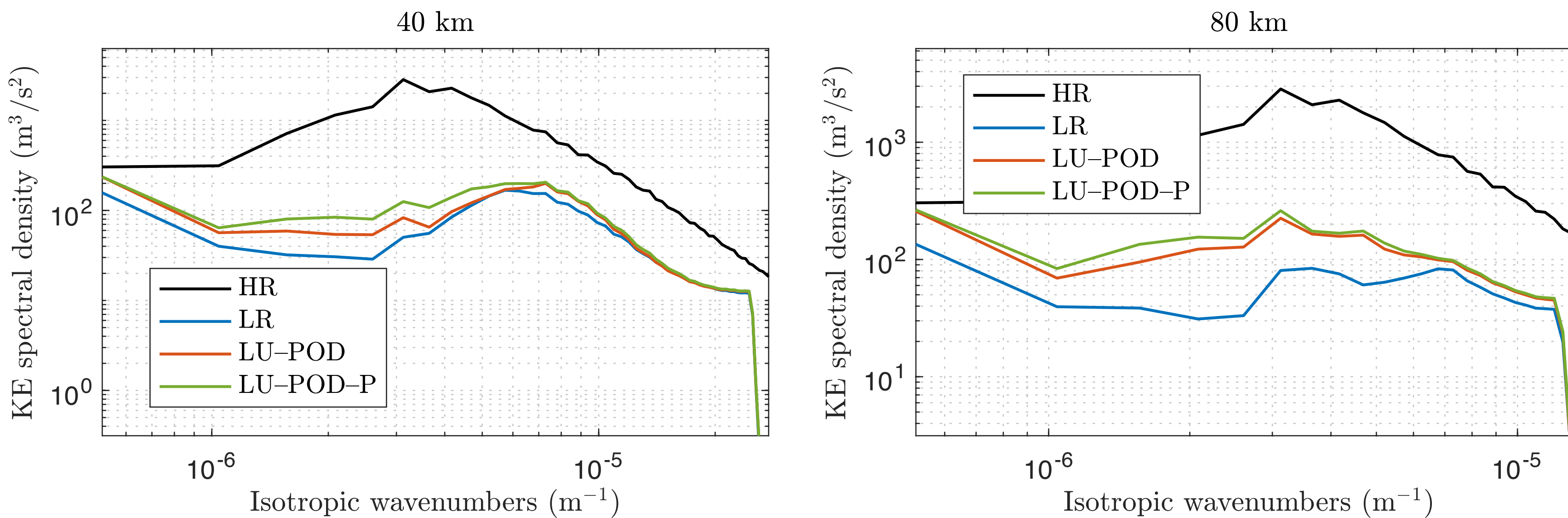


Energy analysis

**Exp.1
(without SST)**



**Exp.2
(with SST)**



**Comparison of
KE spectral
density
averaged in
time (60-75 yrs)
and in layers
for different
coarse models**

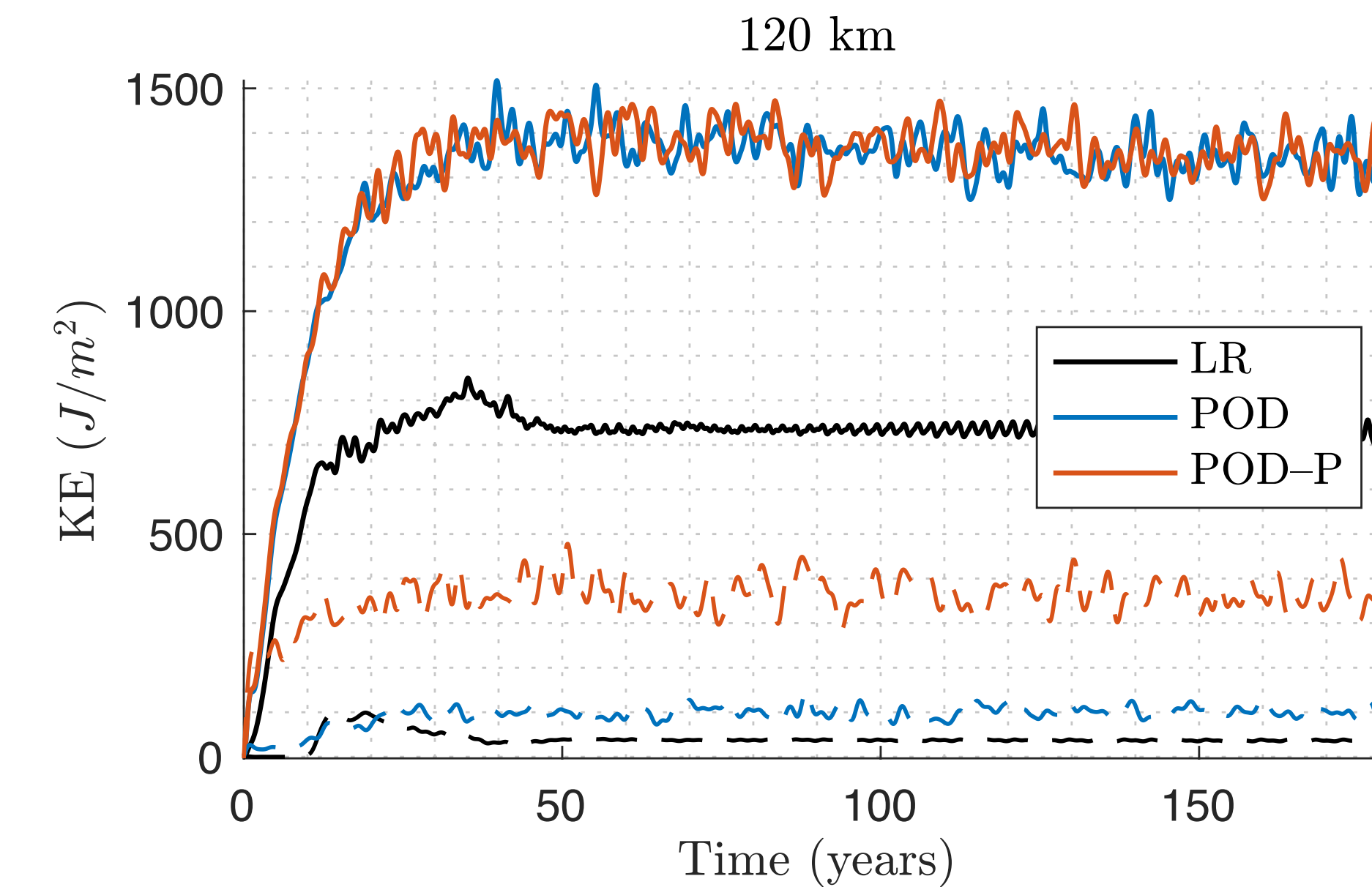
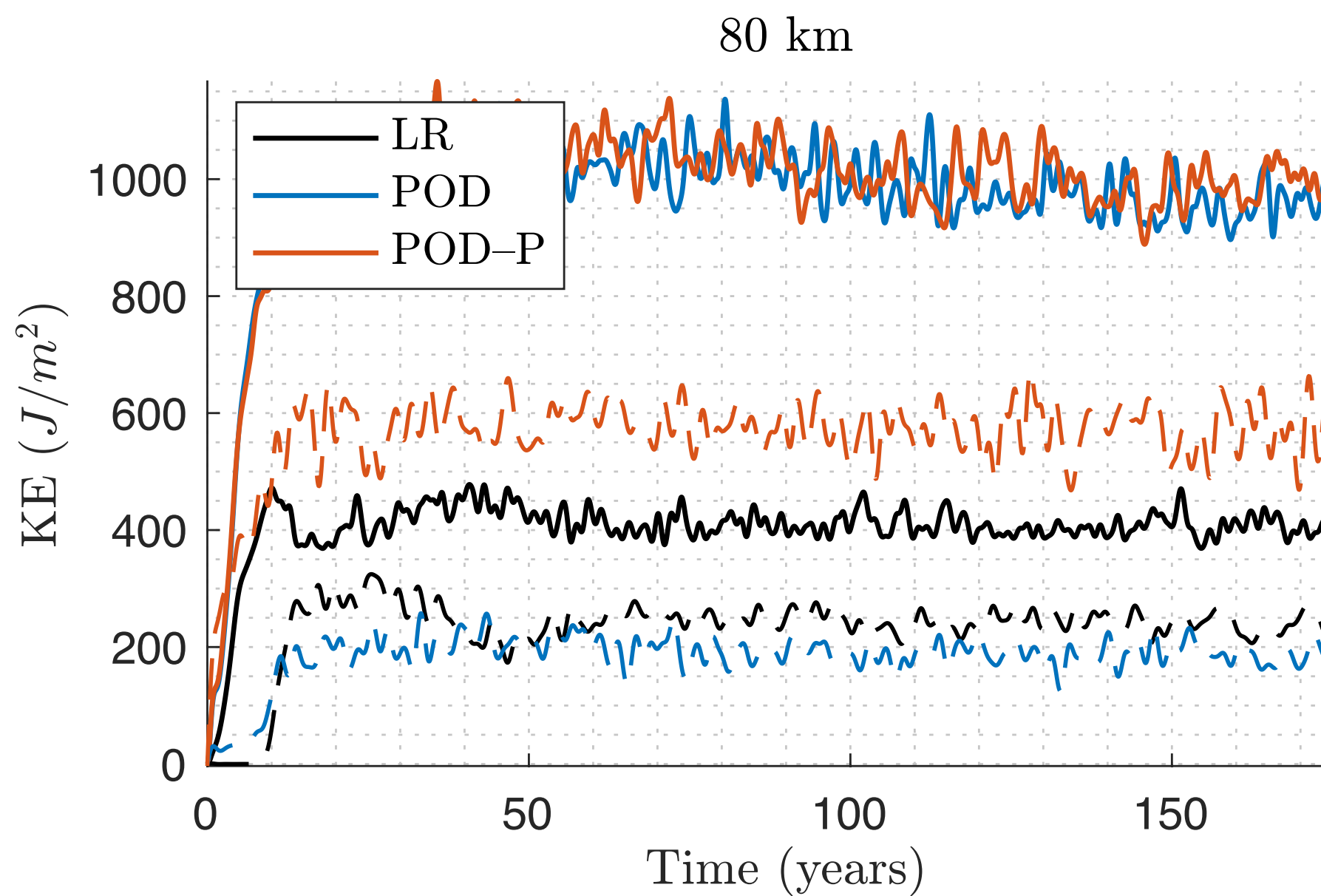
Energy analysis

- KE decomposition

$$\mathbf{u}_k = \bar{\mathbf{u}}_k + \mathbf{u}'_k \quad \text{Low-pass filtering}$$

$$\text{EKE}_k = \frac{\rho_0 H_k}{2} \|\bar{\mathbf{u}}_k\|_A^2 + \frac{\rho_0 H_k}{2} \|\mathbf{u}'_k\|_A^2$$

Standing EKE **Transient EKE**



Comparison of EKE (integrated over layers) for different coarse models (Solid lines – standing EKE, Dashed lines – transient EKE)

Energy analysis

- KE contributions

$$\begin{aligned}
 \text{KE} &= \partial_t \sum_{k=1}^N \frac{\rho_0 H_k}{2} \|\mathbf{u}_k\|_A^2 = -\partial_t \sum_{k=1}^{N-1} \frac{\rho_0 g'_k}{2} \|\eta_k\|_A^2 - \sum_{k=1}^{N-1} \rho_0 g'_k \langle \eta_k, w_k \rangle_A \\
 &\quad + \rho_0 \langle \mathbf{u}_1, \boldsymbol{\tau} \rangle_A - \frac{\rho_0 f_0 \delta_{ek}}{2} \|\mathbf{u}_N\|_A^2 \\
 &\quad + \sum_{k=1}^N \rho_0 H_k \langle \mathbf{u}_k, A_2 \nabla^2 \mathbf{u}_k - A_4 \nabla^4 \mathbf{u}_k \rangle_A
 \end{aligned}$$

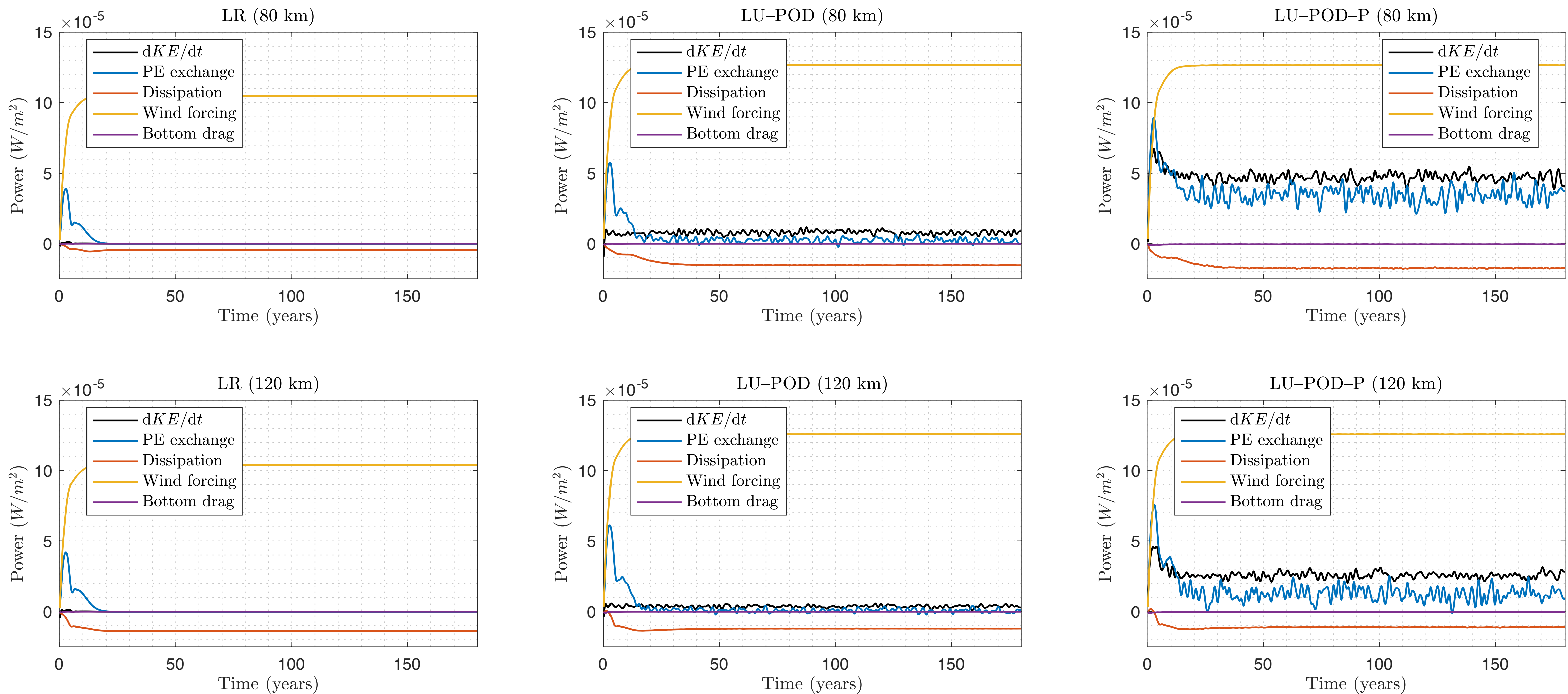
Wind forcing **PE** **Buoyancy forcing**
(= 0 in Exp.1)

Bottom drag

Dissipation

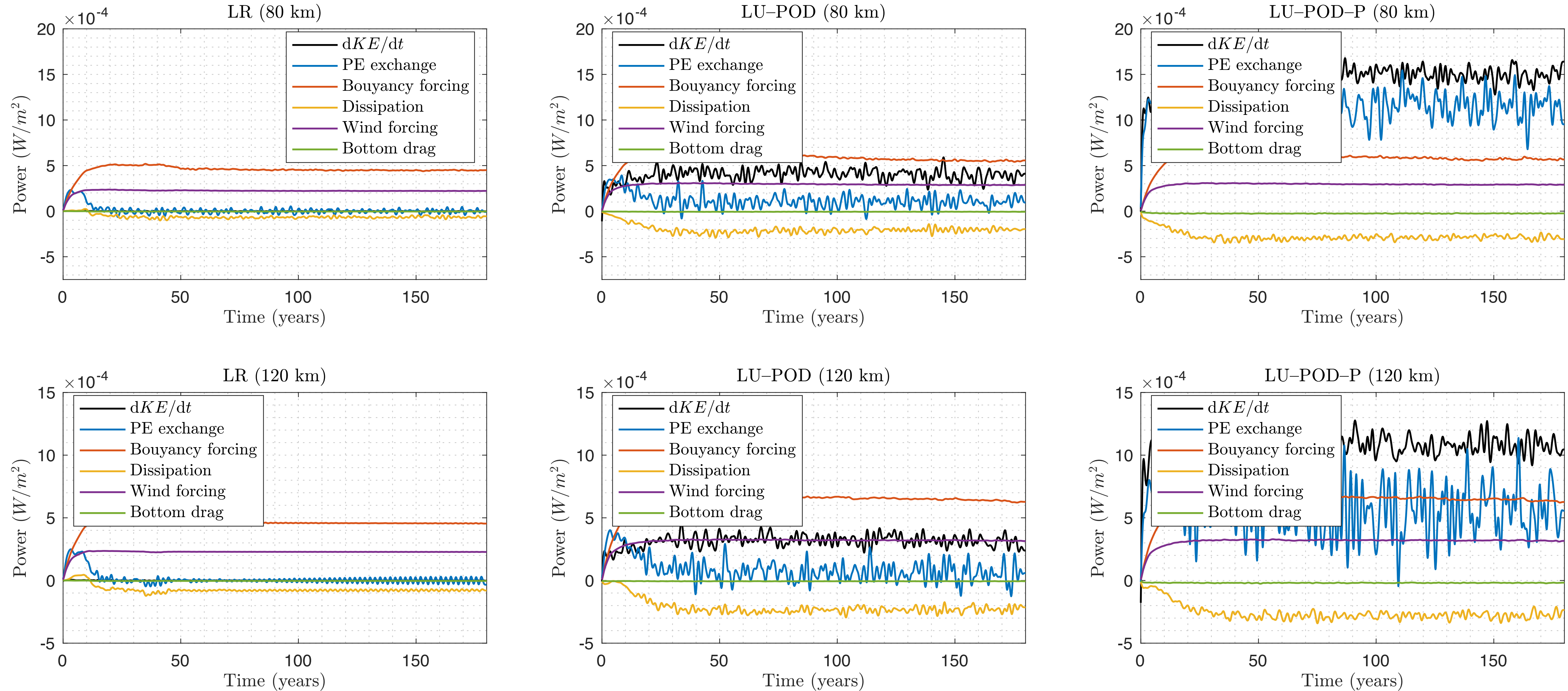
$$\langle f, g \rangle_A = \frac{1}{|A|} \int \int f g \, dA$$

Energy analysis



Comparison of contributions to the rate of KE for different coarse models (Exp.1)

Energy analysis

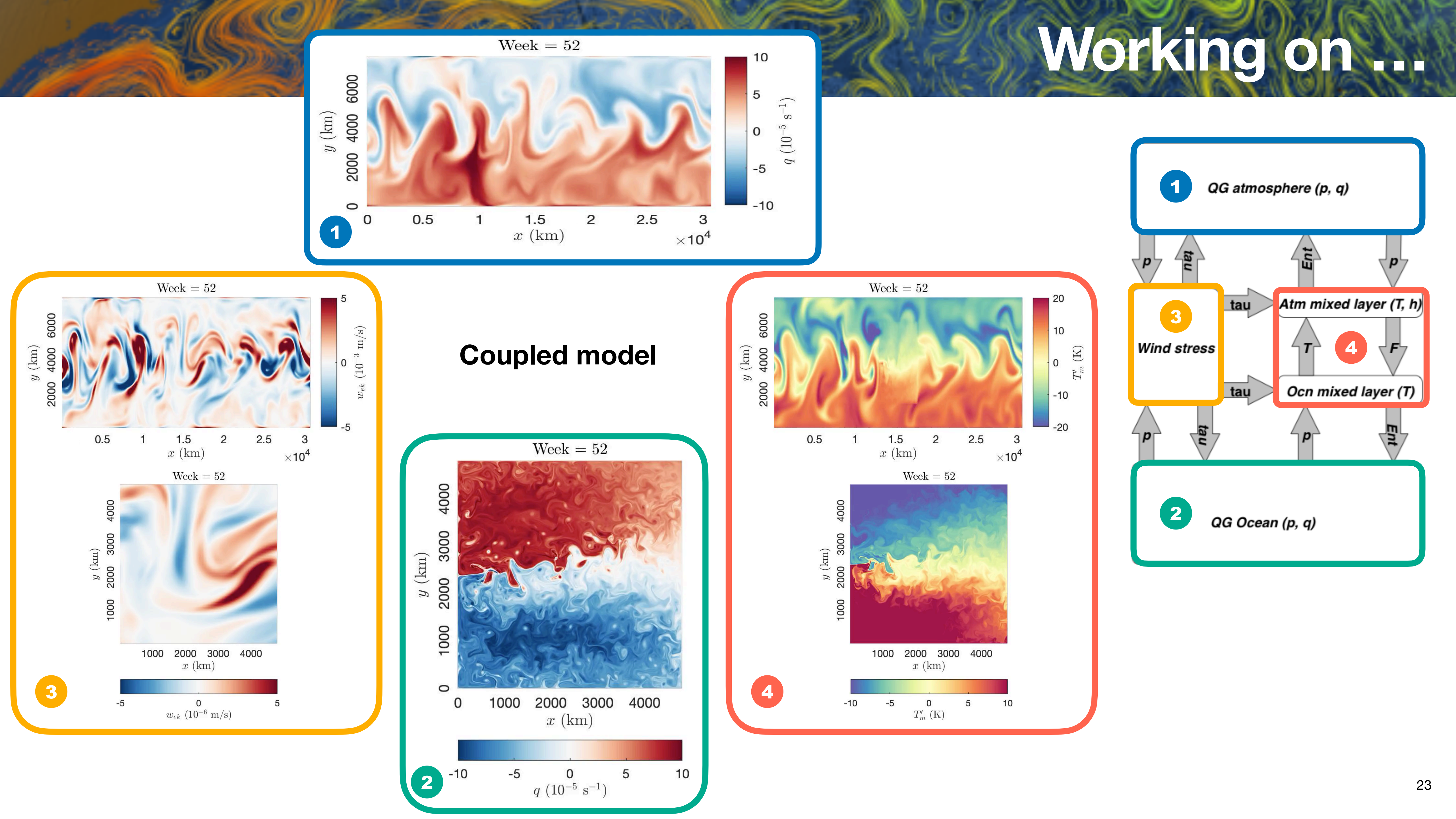


Comparison of contributions to the rate of KE for different coarse models (Exp.2)

Conclusion

- The correction drift is found to be important in reproducing the meandering jet on coarse mesh.
- The non-stationary noise based on the projection method enables us to improve the low-frequency variability of the large-scale circulation.

Working on ...





Thanks for your attention !